THE CARBIDE CONSTITUENT IN IRON-CARBON-SILICON AND RELATED ALLOYS

BY

W. SHEPHERD OWEN.

S Y N O P S I S

Probably the most important of the factors which determine the final structures and properties of cast irons is the nature of the carbide decomposition process. Before any attempt can be made to understand the mechanism of this decomposition it is necessary to know the composition and structure of the carbides present in commercial alloys, which are complex materials containing sulphur, phosphorus, manganese and various gases in appreciable quantities in addition to the basic elements iron, carbon and silicon. In order to attack the problem in a systematic manner it was thought necessary to start by examining relatively simple synthetic alloys. The carbide constituent was first studied in high purity iron-carbon-silicon alloys melted in vacuo. The separate influences of manganese, sulphur and phosphorus on the carbide were then investigated and, finally, each of the main classes of commercial irons was examined and the results interpreted in the light of the knowledge obtained in the study of the high purity alloys. In addition, a number of constituents which previous investigators

have reported as "carbide" phases were investigated.

Microscopic and X-ray diffraction methods have been employed throughout. In order to determine whether or not the additional elements change the composition of the carbide in iron-carbon-silicon alloys the lattice parameters of the carbide structures have been measured to a high degree of accuracy. The methods employed to achieve this accuracy are described. Further information has been obtained by using a new design of back reflection focusing X-ray camera. The theory, construction and operation of this camera are described in an appendix to the thesis.

In conclusion, some ideas concerning the nature of the carbide decomposition process and the relative stability of the carbide in the presence of various proportions of manganese, sulphur and phosphorus, under various temperature conditions, are suggested.

Ph.D. THESIS.

Submitted May 1950.

A C K N O W L E D G E M E N T

I wish to thank

Dr. S. J. Kennett

for his encouragement and interest in the work.

W. Shepherd Owen.

CONTENTS.

[redacted]

I N T R O D U C T I O N

In binary iron-carbon alloys the carbon may occur either as graphite or as a carbide (cementite-Fe_3C) depending upon the composition and the thermal and mechanical treatments to which the alloy has been subjected. It is widely held that graphite is the stable phase at all temperatures and that the carbide, although very persistent under certain conditions, is in fact metastable. However, disagreement with this view has been expressed by certain investigators[1,2,3,4] who consider that there is a high temperature range within which the carbide is the stable phase. In view of the well established fact that the presence of a small quantity of silicon reduces the stability of the carbide it is reasonable to assume that in iron-carbon-silicon alloys graphite is the stable phase at all temperatures.

White irons are manufactured under conditions which ensure that all the carbon is present in the form of carbide and as these irons form an important class of engineering materials a knowledge of the crystal structure of this carbide is of interest. Malleable irons are produced from selected white irons by an annealing process which causes the decomposition

of the carbide to the more stable graphite. The resistance of the carbide to decomposition, at a particular annealing temperature, is greatly affected by the proportions of silicon and minor constituents present in the alloy. Further, the metallographic form of the graphite ultimately produced is also influenced by the composition. For example, it has been shown by Morrough[5] that if the sulphur present is in excess of that required to form manganese sulphide (MnS) (as in White-heat malleable iron) the graphite is present as spherulitic nodules (Figure 1.); whilst, if there is excess manganese (as in Black-heat malleable iron) the graphite occurs as aggregates of small flakes having no particular orientation to one another (figure 2). Clearly, a knowledge of the crystal structure of the carbide and the influence of the minor constituents on this structure is a prerequisite of any hypothesis aimed at an understanding of the decomposition process.

Interest in the problem is intensified by recent advances which have been made in the metallography of grey cast irons. Eash[6] showed that the type of graphite structure generally known as supercooled graphite (figure 3) - classified by the American Society for

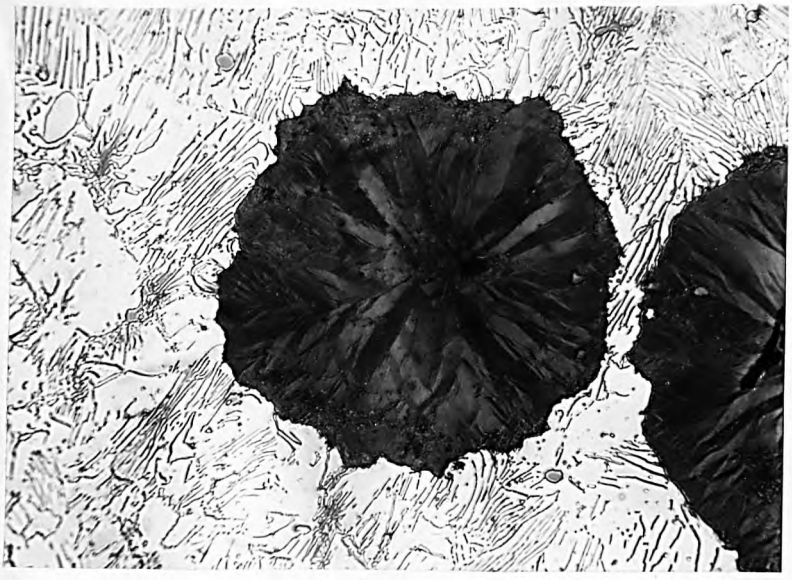

Figure. 1. Sperulitic Nodular Graphite in Malleable Iron. x 2 5 0 .

Figure. 2. Flake Aggregate Graphite in Malleable Iron. x100.

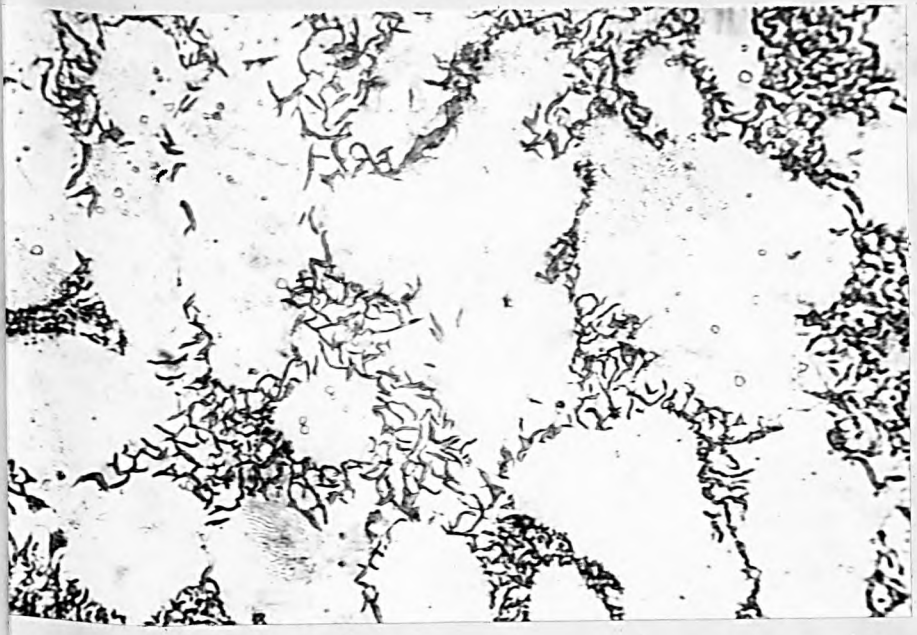

Figure. 3. Supercooled Graphite - Type D.
x250.

Testing Materials[7] as Type D - is formed by the decomposition of carbide in the solid state during the cooling of the iron from the melt. This conclusion, which was later confirmed by the more precise experimental work of Morrough and Williams,[8] has necessitated a reconsideration of the theory of graphite flake formation, In addition, a new class of iron in which much of the graphite is in a nodular form, similar to that found in white-heat malleable iron, has recently been developed; these irons contain alloy additions such as nickel and cerium in controlled amounts.[9] It is supposed that the specific graphite structures obtained are produced by decomposition of the carbide during cooling from the melt. Although, a study of the influence of such alloy additions does not come within the scope of the work to be described in this thesis, a knowledge of the structures of the carbides in the basic alloys provides a starting point for such work.

The object of the present investigation was to determine the crystal structure of the carbide constituents in various commercial irons and the influence of minor constituents, manganese, sulphur and phosphorus, on those structures. To do this in a systematic manner it was necessary to examine the

carbide in high purity iron-carbon-silicon alloys, and then to determine the effect of separate additions of manganese, sulphur and phosphorus, before attempting to determine the structure of the carbide constituents in commercial irons. The microscopic studies of Marles[11] and of Hurst and Riley[12] have revealed the presence of constituents, in certain special iron-carbon-silicon alloys (of commercial purity), which they considered to be "carbides" and these also have been examined.

All the alloys used in the investigation were subjected to a detailed microscopic examination. The crystal structures of the carbide constituents were determined by a Debye-Scherrer X-ray powder method. The lattice dimensions of all these structures were measured and sensitive methods of detecting changes in these parameters in the presence of minor constituents were employed. Other constituents present in the alloys were investigated by a Debye-Scherrer back reflection focusing method applied to the surface of the microspecimens. As the same experimental methods were used for all the alloys these methods will be described first.

This study has provided information which enables certain tentative suggestions to be made regarding the

nature of the carbide-graphite change during annealing, and the manner in which the minor constituents influence this reaction and these ideas are set out at the end.

PREVIOUS INVESTIGATIONS

The crystal structure of cementite in binary iron-carbon alloys has been established by the work of Westgren,[13] Westgren and Phragmen,[14] Hendricks,[15] Lipson and Petch,[16] and Hume-Rothery, Raynor and Little.[17] With the exception of Lipson and Petch who prepared their powder synthetically, all these investigators used cementite extracted from plain carbon steels containing the usual small quantities of silicon, manganese, sulphur and phosphorus present in these commercial alloys. The structure is fully described by Lipson and Petch, who state it to be orthorhombic with 12 iron atoms and 4 carbon atoms in the unit cell. The Space Group is D_{2h}^{16} which is equivalent to V_h^{16}, the iron atoms being at positions

$$\left.\begin{array}{l} u, v, \tfrac{1}{4} \\ (\tfrac{1}{2}-u), (\tfrac{1}{2}+v), \tfrac{1}{4} \\ u, v, \tfrac{3}{4} \\ (\tfrac{1}{2}+u), (\tfrac{1}{2}-u), \tfrac{3}{4} \end{array}\right\} \quad \begin{array}{l} u = -0.167 \\ v = 0.040 \end{array}$$

$$\left.\begin{array}{l} x, y, z \\ x, y, (\tfrac{1}{2}-z) \\ (\tfrac{1}{2}-x), (\tfrac{1}{2}+y), z \\ (\tfrac{1}{2}-x), (\tfrac{1}{2}+y), (\tfrac{1}{2}-z) \\ \bar{x}, \bar{y}, \bar{z} \\ \bar{x}, \bar{y}, (\tfrac{1}{2}+z) \\ (\tfrac{1}{2}+x), (\tfrac{1}{2}-y), \bar{z} \\ (\tfrac{1}{2}+x), (\tfrac{1}{2}-y), (\tfrac{1}{2}+z) \end{array}\right\} \quad \begin{array}{l} x = 0.333 \\ y = 0.183 \\ z = 0.065 \end{array}$$

whilst the carbon atoms are at positions equivalent to those of the first four iron atoms with

$$u = 0{\cdot}47$$

$$v = 0{\cdot}14$$

The dimensions of the unit cell were determined incorrectly by Lipson and Petch. More accurate work by Hume-Rothery, Raynor and Little later showed them to be

a	= 4·5155	Å
b	= 5·0773	Å
c	= 6·7265	Å
a/b	= 0·88934	
c/b	= 1·32481	

Very little data are available for alloys containing carbide in the presence of an appreciable quantity of silicon. Westgren and Phragmèn[14] (1922), during the course of an investigation of the crystal structure of cementite in steels, examined a "white annealing iron" and failed to detect any difference between the carbide from this alloy and cementite from steels. However, the accuracy of this early work was not very great, as has been shown by the more recent work on the parameters of the unit cell of cementite, and it would be unwise to make any deductions from this

isolated determination. The only other information which is available is contained in a paper by Schwartz, Van Horn and Junge[10] who obtained back reflection Debye-Scherrer photographs of a white iron containing 2·3% carbon and 1·2% silicon quenched from various annealing temperatures. These showed a few faint lines, amongst the broadened austenite and ferrite lines, which they decided were produced by cementite and, although they did not index the lines and were only able to measure the interplanar spacing to about $\pm$ ·01 Å, they stated that: "The cementite reflections in the pattern of the specimen quenched from 888°C possibly indicated a slight contraction of the cementite lattice as determined from the pattern of white cast iron. A lattice contraction would perhaps signify a simple substitutional introduction of carbon atoms". When these results are examined from the stand point of our present day knowledge of X-ray technique they appear quite unreliable and the deductions made from them are thus, without further investigation, unacceptable.

No information is available concerning the quaternary alloys.

Evidence of the nature of the carbide constituents based upon experimental data other than that obtained by X-ray methods will be considered later under the appropriate headings.

THE EXPERIMENTAL METHODS

MICROSCOPIC EXAMINATION

In the early stages of the investigation the alloys were polished with chromic oxide followed by magnesia powder. The hard carbide constituents invariably stood in relief from the softer matrix and thus it was difficult to obtain suitable photographs of the micro-structures. The problem was solved by using diamond dust. The specimens were ground down to a 3/0 emery paper and then polished on a 4" diameter wheel over which was stretched a Selvyt cloth impregnated with 15 mg. of diamond dust (less than 1 μ) and then damped with a few drops of paraffin. At 100 R.P.M. the average specimen was polished within one half to two minutes.

In general 3% alcoholic nitric acid was used as an etchant, although for some purposes picric acid etchants or heat tinting was necessary. The high silicon alloys (greater than 10% silicon) were etched in a solution containing one part of nitric acid, one part of hydrofluoric acid and six parts of water. If the specimen is then washed in alcohol and dried immediately a "barley-shell" structure is observed

which is due to a deposited film and is not the true structure of the alloy. 18.19.20. It was found that this film formation could be prevented by washing the specimen for 3 to 5 minutes in warm water before transferring to the alcohol bath.

CHEMICAL ANALYSIS

All the analyses were performed by standard methods.

X-RAY DIFFRACTION WORK

The Debye-Scherrer Powder Method

When prepared by crushing the ingot, with the exception of those containing more than 10% silicon, the alloy specimens failed to yield X-ray diffraction patterns suitable for detailed study of the carbide. This result was anticipated, since the large number of weak reflections from the low symmetry carbide structures are further weakened by dilution of the specimen by the other constituents present. It was therefore necessary to extract the carbides from the alloys. Numerous methods of extracting carbides from plain carbon and alloy steels have been described. These may be classified as :-

1. Treatment with a cold solution containing:

Cuprous Chloride	90 grms.
Potassium chloride	60 grms.
Hydrochloric acid	32 grms.
Water	500 cc.

2. Treatment in dilute hydrochloric acid solutions.[21]
3. Anodic treatment in dilute hydrochloric acid[17,22]
4. Treatment with chlorine gas[23,24,25]
5. The Alcoholic iodine method[26,27,28,29]
6. The Aqueous Iodine method[30,31,32,33]
7. Cuprous chloride two-solution electrolytic methods[34.]

Methods 1,3,6 and 7 were tried on a commercial white iron and a commercial grey iron. In all cases satisfactory diffraction photographs were obtained from the powders which remained after treatment. The quickest and simplest method was by electrolytic treatment in a dilute solution by hydrochloric acid and this was used on all subsequent occasions. The specimen, suspended by means of a platinum wire, was made the anode of an electrolytic cell, the cathode being a copper sheet and the electrolyte 4% hydrochloric acid. After 12 hours attack at a current density of 20-22 ma per sq. cm. the coherent adhesive layer of

insoluble constituents on the surface of the specimen was removed with a pen-knife, washed in hot dilute hydrochloric acid, hot water, cold water and alcohol successively, and finally dried in an air oven at less than 100°C. The dried powder was passed through a 100 mesh sieve to remove any coarse particles and then the fines were separated through a sieve of 240 mesh. The powder, -100 + 240 mesh, was packed into thin walled cellophane capillary tubes of 0·4 mm. internal diameter.

The specimens were exposed in a 19cm Debye-Scherrer X-ray camera. The details of the construction and operation of this camera have been described by Bradley[35] The camera is illustrated diagrammatically in Appendix 1. For the majority of the exposures filtered cobalt radiation was used. In a few instances iron radiation, filtered by manganese, was found to give better results.

As the validity of the conclusions drawn from this work is largely dependent upon the accuracy with which the diffraction angles have been measured, and as this in turn is dependent upon the value adopted for the camera constants, considerable attention was paid to the question of determining these constants

with the greatest possible accuracy. The arc distance between the low angle knife edges was determined by measuring the linear separation and the camera diameter with micrometers which had been standardised against "Matrix" blocks. The measurement of the angle subtended at the centre of the camera by the high-angle knife edges ($4\theta_K$) presented more difficulty. Two methods were used, (a) calculation from direct micrometer measurements of the linear distance between the knife edges and the diameter of the camera (b) indirect estimation from diffraction data obtained by using quartz as a standard substance. The accuracy of method (b) depends upon the values adopted for the lattice spacings in quartz and the proportionality function used to eliminate the systematic experimental error. A table of the angles of diffraction from quartz using Copper $K\alpha$ radiation at 18°C was given by Bradley and Jay[36], but was found to be based upon incorrect values for the lattice spacings. A corrected table was published by Lipson and Wilson[37] and these values were adopted in the present investigation. The values of θ_K determined in this manner show a drift with θ which is due to the systematic error arising from certain experimental causes, the more

important being absorption by the specimen, displacement of the specimen from the centre of the camera and eccentricity during the rotation of the specimen. Bradley and Jay showed that these errors in θ_K were very nearly proportional to $\frac{\sin 2\theta}{2\theta}$ for values of θ greater than 60^0 and thus may be eliminated by plotting θ against this function and extrapolating to $\frac{\sin 2\theta}{2\theta} = 0$. Two cameras were used in the present work and the values of the constant θ_K, determined by the two methods, are set out in Table 1. These values are the average values of three determinations in each case.

TABLE 1.

	Camera 1.	Camera 2.
θ_K by direct measurement	$85{\cdot}323^0$	$85{\cdot}365^0$
θ_K, Bradley and Jay method	$85{\cdot}281^0$	$85{\cdot}302^0$

The agreement between these results is not as good as might be expected. This fact has been noted by other investigators[37,38] and it is generally agreed that the direct measurement method is more likely to give the correct value[38].

The question of the relationship between the

diffraction angles and the systematic experimental error in Bradley type cameras was reinvestigated from a theoretical standpoint by Taylor and Sinclair[39] and experimentally by Nelson and Riley[38]. They concluded that all the errors, with the exception of the absorption error, could be completely eliminated by proper construction of the camera and careful setting up of the specimen. The error in the length of the cube edge of the unit cell of a cubic structure due to absorption by the specimen was shown to be proportional to $\frac{1}{2}\left[\cot\theta + \frac{1}{2}\left(\frac{\cos^2\theta}{\sin\theta} + \frac{\cos^2\theta}{\theta}\right)\right]$ for a "medium thickness undiluted" specimen of the type used in the present work. Unlike the Bradley-Jay function, this may be used for the whole range of θ values recorded on the film. This provides a method of testing the accuracy of the value of θ_K, for an inaccuracy will result in a deviation from a straight line plot and, further, the sign of the error in θ_K may be deduced from the nature of the deviation. This test was applied using a sample of pure iron and another of pure silicon. These were set up with great care to eliminate the geometric errors and exposed in the usual manner. The error in the length of the side of the unit cell, $\frac{\Delta a}{a}$, was plotted

against $\frac{1}{2}\left[\cot\theta + \frac{1}{2}\left(\frac{\cos^2\theta}{\sin\theta} + \frac{\cos^2\theta}{\theta}\right)\right]$ and the form of the plot was examined.

With both cameras good straight line plots were obtained when the values for θ_K obtained by direct measurement were used, whilst the values obtained by the quartz method resulted in small deviations. The direct measurement values have been used in all the subsequent calculations.

In all cases, the correction for film shrinkage has been made by the method of Lipson and Wilson[37] as the values of θ have been calculated from the formula:

$$\theta = \theta_K \cdot \frac{S}{S_K}$$

where S = Arc distance between the diffraction lines.

S_K = Total distance of film exposed + arc distance between low angle knife edges.

THE BACK REFLECTION FOCUSING CAMERA

It was thought desirable to examine the constituents other than carbide, which were present in the alloy. To do this by the Debye - Scherrer method described in the previous section it was necessary to crush the small ingots to powder. The diffraction photographs obtained

showed extremely broad lines quite unsuitable for further study; much of the broadening being produced by the strains induced in the powder by the crushing operation. When attempts were made to remove the strain (and hence sharpen the lines) by annealing the powders it was found that breakdown of the carbide occurred before any appreciable stress-relief was effected. Thus, in order to examine these other constituents, it was necessary to devise a method which would produce a diffraction pattern directly from the lump specimen. To do this a new type of back reflection focusing Debye-Scherrer camera was designed and constructed. This camera may be used for the X-ray examination of any microscopic metallographic specimen of a normal size. Details of design and operation, together with an example of the method of calculating lattice parameters from the results obtained are given in Appendix 1.

THE CARBIDE CONSTITUENT IN IRON-CARBON-SILICON ALLOYS.

I N T R O D U C T I O N

It is evident that the carbide phase in iron rich iron-carbon-silicon alloys is closely related to the cementite (Fe_3C) phase in iron-carbon alloys, but the precise composition has been the subject of much speculation. The existence of complex carbides of iron and silicon has been assumed by numerous investigators of the ternary system, including Honda and Murakami,[40] Hanson,[41] and Sawamura,[42] Scheil[43.44] concluded that the carbide phase does contain silicon, although he considered the data insufficient to substantiate the deductions implicit in the experimental results of Kriz and Poboril[45] that it contained as much as 4·5%. Kriz and Poboril[45.46] also advanced the metallographic evidence that "carbide in iron-carbon-silicon alloys - when etched with hot alkaline solution of sodium picrate - is coloured considerably less than cementite (Fe_3C)". This view that silicon dissolves in the carbide, led the author to attempt to interpret certain unusual microstructures observed by Marles,[11] on the assumption that silicon is capable of segregating within the carbide phase.[47]

It was pointed out by Petch[22] that there must be direct iron-iron bonding in the cementite structure, each iron atom having eleven or twelve almost equidistant iron neighbours. The structure is considered as "consisting essentially of a framework of closely packed iron atoms held together by metallic bonding, with the small carbon atoms in the largest interstices, the carbon atoms also being held in position by bonding which has a certain amount of metallic nature, and the whole structure being more dominated by iron-iron than by iron-carbon bonding". On this view the substitution of iron atoms by other atoms of favourable size factor and electron structure is possible. It is well established that chromium or manganese atoms can replace iron atoms to a limited extent.[21] As silicon has a favourable size factor to replace iron in a structure in which the interatomic distances are of the magnitude found for the iron-iron distances in cementite, it is possible that such substitution does occur. It would be expected that alloying of this nature would be accompanied by an appreciable change in the dimensions of the unit cell in view of the marked difference in atom size. It would not be possible, however, to deduce the amount of silicon entering the structure from such

measurements since for example, contrary to expectations, the substitution of iron atoms by the larger chromium atom causes a decrease in the size of the cell.

EXPERIMENTAL

A total of eight ingots of iron-carbon-silicon alloys were cast from high purity materials. When preparing these it was necessary to satisfy several conflicting conditions in the best possible manner: Namely, the alloy should contain the maximum amount of silicon and carbon, the rate of cooling should be as slow as possible to reduce the internal strain produced during cooling, and the carbon should appear as carbide. The extracts from each specimen was examined. Some contained graphite as well as carbide and, as the reflections from graphite are much stronger than those from carbide, the diffraction patterns were considered unsuitable for detailed examination. The patterns from some other samples showed rather diffuse lines unsuitable for accurate measurement. Attempts to sharpen the lines by annealing these specimens were not successful as considerable decomposition took place and the carbide lines, although somewhat sharpen, were very faint due to dilution of the specimen with graphite and ferrite. Only those specimens with massive carbide gave

satisfactory diffraction photographs; the best results being obtained from those prepared under controlled rates of cooling from the melt. Two specimens were studied in detail together with a specimen of hyper-eutectoid steel of similar composition to that used by Hume-Rothery, Raynor and Little when they determined the parameters of cementite to a high degree of accuracy.[17]

Specimen 1 (Film 353)

A hyper-eutectic steel containing, carbon 1·00%, manganese 0·53%, silicon 0·15%, sulphur 0·044%, phosphorus 0·041%, nickel 0·17%, chromium 0·05%. It was annealed for 5 hours at 900°C, cooled in the furnace, and then had a normal pearlitic structure with a cementite network at the crystal boundaries.

Specimen 2 (Film 383)

A sample prepared from high purity materials:-*

Hilger iron, J.M.845.

Silicon, (St.Lawrence Alloys and Metals Ltd., Quebec), containing 99·92% silicon, the major impurity being 0·022% aluminium.

Carbon, graphite with an ash content of 0·07%.

The charge (75 grams) was melted in a recrystallised alumina crucible by means of a coil energised by a valve

* The analyses of these materials is given in Appendix 3.

oscillating high frequency unit. The experimental arrangement is shown diagrammatically in figure 4. A pressure of less than 10^{-3} mm. mercury was maintained throughout the melting and cooling cycle, except for a period of about 3 minutes duration when the pumping speed of the condensation pump was insufficient to handle the large volume of gas produced in the early stages of the melting. The superheated melt was maintained under vacuum for 45 minutes until the surface was clean and all evidence of gas evolution had ceased. At the end of this period the high frequency current was switched off and after 10 minutes the vacuum was broken, by which time the specimen had cooled to a temperature of less than 200°C.

A total of five melts with different silicon contents were treated in this manner, but it was impossible to suppress the formation of graphite in alloys containing more than 2·0% silicon. The alloy chosen for further study contained 1·95% silicon and 2·51% carbon. Metallographic examination of the unetched specimen showed this alloy to be almost completely free from inclusions, and on etching the carbide was seen to be massive although there was considerable variation in the size of the carbide

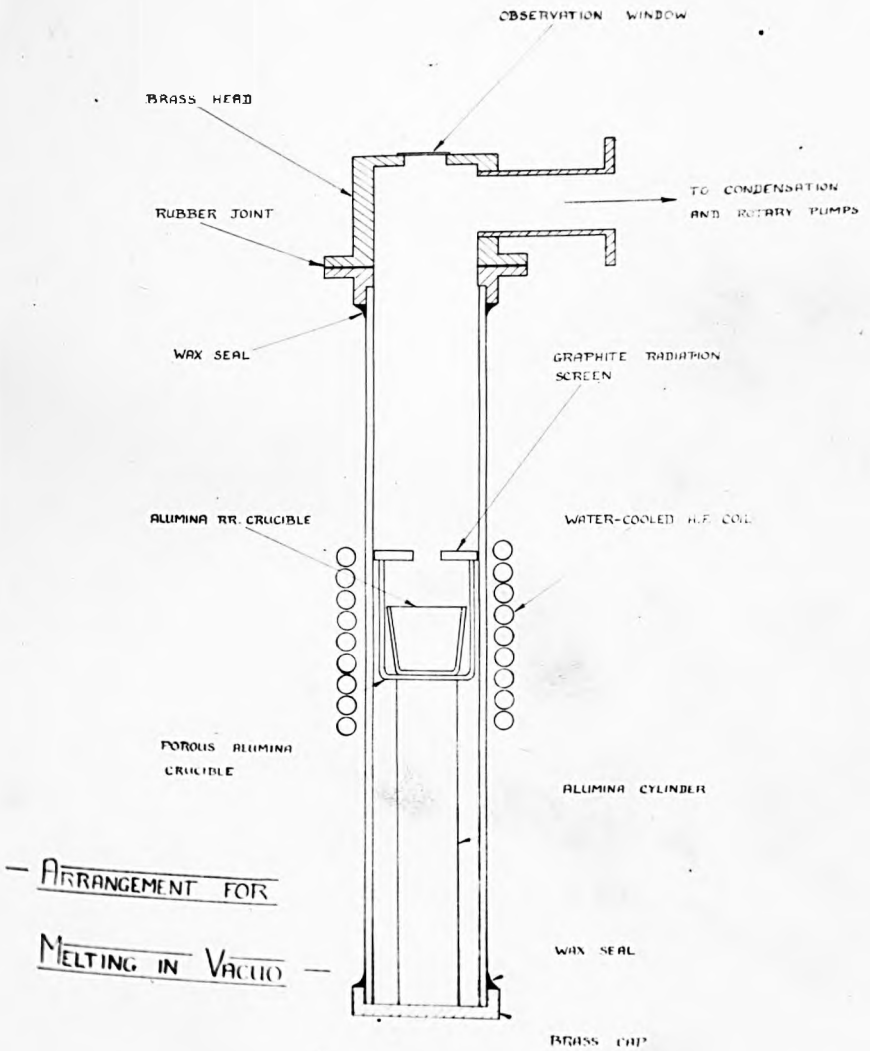
OBSERVATION WINDOW
BRASS HEAD
TO CONDENSATION
AND ROTARY PUMPS
RUBBER JOINT
WAX SEAL
GRAPHITE RADIATION
SCREEN
ALUMINA RR. CRUCIBLE
WATER-COOLED H.F. COIL
POROUS ALUMINA
CRUCIBLE
ALUMINA CYLINDER
WAX SEAL
BRASS CUP
ARRANGEMENT FOR
MELTING IN VACUO

Figure. 4.

areas from the outside to the centre of the specimen. An idea of the extent of the variation may be obtained by comparing figures 5 and 6.

Specimen 3 (Film 379)

Attempts were made to increase the rate of cooling of the specimen by breaking the vacuum at an earlier stage and blowing cold air onto the surface of the metal. This treatment produced considerable surface oxidation without enabling an appreciable increase in silicon content to be made.

In order to produce a suitable alloy with a higher silicon content several melts were made in glazed silica crucibles heated in air by means of a graphite sleeve within a high frequency coil. The metal was cast into the form of a ¼" diameter rod in a cast iron chill mould. The materials used for these melts were the same as for specimen 3, except that an electrolytic iron containing less than 0·05% total impurities, other than carbon, silicon and oxygen, was employed. The alloy selected contained 3·14% silicon and 3·49% carbon. A metallographic examination revealed remarkably few inclusions and a rather broken up carbide structure (figure 7).

Two samples of extracted powder from each specimen were examined and each film was measured at least twice.

Figure. 5. Carbide in High Purity Fe-C-Si Alloy.
Specimen 2. x600.

Figure. 6. Carbide in High Purity Fe-C-Si Alloy.
Specimen 2. x600.

Figure. 7. Carbide in High Purity Fe-C-Si Alloy. Specimen. 3.

It was clear from a cursory examination of the films that there was very little difference between the pattern from the cementite of specimen 1 and the carbides from the alloys containing silicon. Hence an attempt was made to index the lines by comparing the $\sin^2\theta$ values with a list of $\sin^2\theta$ values for all possible planes of the cementite (Fe_3C) structure calculated from the values of the dimensions of the unit cell given by Hume-Rothery, Raynor and Little. These calculated values are given in Table 1, Appendix 2. It was found that all the lines on all the films could be indexed with certainty in this way. On careful visual comparison the line spacing on all four films appeared identical. Some of the lines were too faint and others, where overlapping occurred, too diffuse to allow accurate measurement and thus a selection had to be made. In the 1940 investigation by Lipson and Petch twenty six lines in the θ range 20° to 35° were used for intensity measurements. All these were clear and sharp on the films obtained in the present investigation and so were measured. Later Petch used five lines in the range $\theta = 47^\circ$ to $\theta = 51^\circ$ and in the very accurate work of Hume-Rothery, Raynor and Little eight lines in the θ range 69° to 78° were measured. On films 1 and 2 all the Petch and

Hume-Rothery lines were clear and were measured without difficulty, while on film 3 the 025 line in the Petch range was too faint to measure and only two Hume-Rothery lines were sufficiently clear to be useful. The results are set out in detail in table 1, Appendix 3. The match between the present experimental values of $\sin^2 \theta$ and those calculated from the data given by Hume-Rothery, Raynor and Little was so close for the high angle lines that there seemed little point in adjusting the dimensions in order to obtain an even better match. However, as only a few high angle lines were available on film 3, a further examination of the differences in the values of $\sin^2 \theta$ was felt to be desirable. The difference, $\Delta \sin^2 \theta$, was therefore plotted against a function linearly proportional to the systematic error in $\sin^2 \theta$. As most of the lines lay below 60^0, the Bradley-Jay function, $\cos^2 \theta$, could not be used. It has already been shown that the Taylor-Sinclair function for the relationship between θ and the error in the length of the cube edge of the unit cell of a cubic structure is applicable to the present experimental arrangement. The low angle limit of proportionality of this function was found to be about 30^0. From this

proportionality relationship a function proportional to the error in $\sin^2\theta$ can be derived in the following manner: From the work of Taylor and Sinclair we have

$$\frac{\Delta a}{a} \propto \frac{1}{2}\left[\cot\theta + \frac{1}{2}\left(\frac{\cos^2\theta}{\sin\theta} + \frac{\cos^2\theta}{\theta}\right)\right] \quad \ldots\ldots\ldots (1)$$

where a = length of cube edge of unit cell of a cubic structure.

If d = crystallographic plane spacing

$$\frac{\Delta d}{d} \propto \frac{\Delta a}{a}$$

hence

$$\frac{\Delta d}{\alpha} \propto \frac{1}{2}\left[\cot\theta + \frac{1}{2}\left(\frac{\cos^2\theta}{\sin\theta} + \frac{\cos^2\theta}{\theta}\right)\right] \quad \ldots\ldots\ldots (2)$$

which relationship may now be applied to any structure. From the Bragg equation

$$\lambda = 2d\sin\theta$$

squaring and taking logarithms

$$2\log d = -\log\sin^2\theta + 2\log\left(\frac{\lambda}{2}\right) \ldots\ldots$$

If we assume there is no error in the value of the wavelength, the term $2\log\left(\frac{\lambda}{2}\right)$ may be treated as a constant. Then differentiating

$$2\frac{\Delta d}{d} = -\frac{\Delta\sin^2\theta}{\sin^2\theta} \quad \ldots\ldots\ldots\ldots\ldots (3)$$

Combining equations (2) and (3)

$$\frac{\Delta \sin^2\theta}{\sin^2\theta} \propto \frac{1}{2}\left[\cot\theta + \frac{1}{2}\left(\frac{\cos^2\theta}{\sin\theta} + \frac{\cos^2\theta}{\theta}\right)\right]$$

Hence

$$\Delta \sin^2\theta \propto \left[\sin 2\theta + \sin^2\theta\left(\frac{\cos^2\theta}{\sin\theta} + \frac{\cos^2\theta}{\theta}\right)\right]$$

This form of the function was considered most convenient as tables of $\sin 2\theta$, $\sin^2\theta$ and $\frac{1}{2}\left(\frac{\cos^2\theta}{\sin\theta} + \frac{\cos^2\theta}{\theta}\right)$ are available. The function may be used for θ values from 90° to about 37°. Below this value the function, when equated, gives two solutions and is thus unsuitable. The plots of $\Delta \sin^2\theta$ against $\left[\sin 2\theta + \sin^2\theta\left(\frac{\cos^2\theta}{\sin\theta} + \frac{\cos^2\theta}{\theta}\right)\right]$ showed some scatter, but the best straight line in each case passed through the origin at $\theta = 90^\circ$, (figure 8), thus demonstrating that the difference between the experimental values and those predicted from the chosen parameters disappears when the systematic experimental error is eliminated at $\theta = 90^\circ$.

The overlapping high angle lines 136 α_1 and 251 α_2 provide a means of testing the accuracy of the chosen axial ratio c/b as the separation of these lines is very sensitive to a change in this

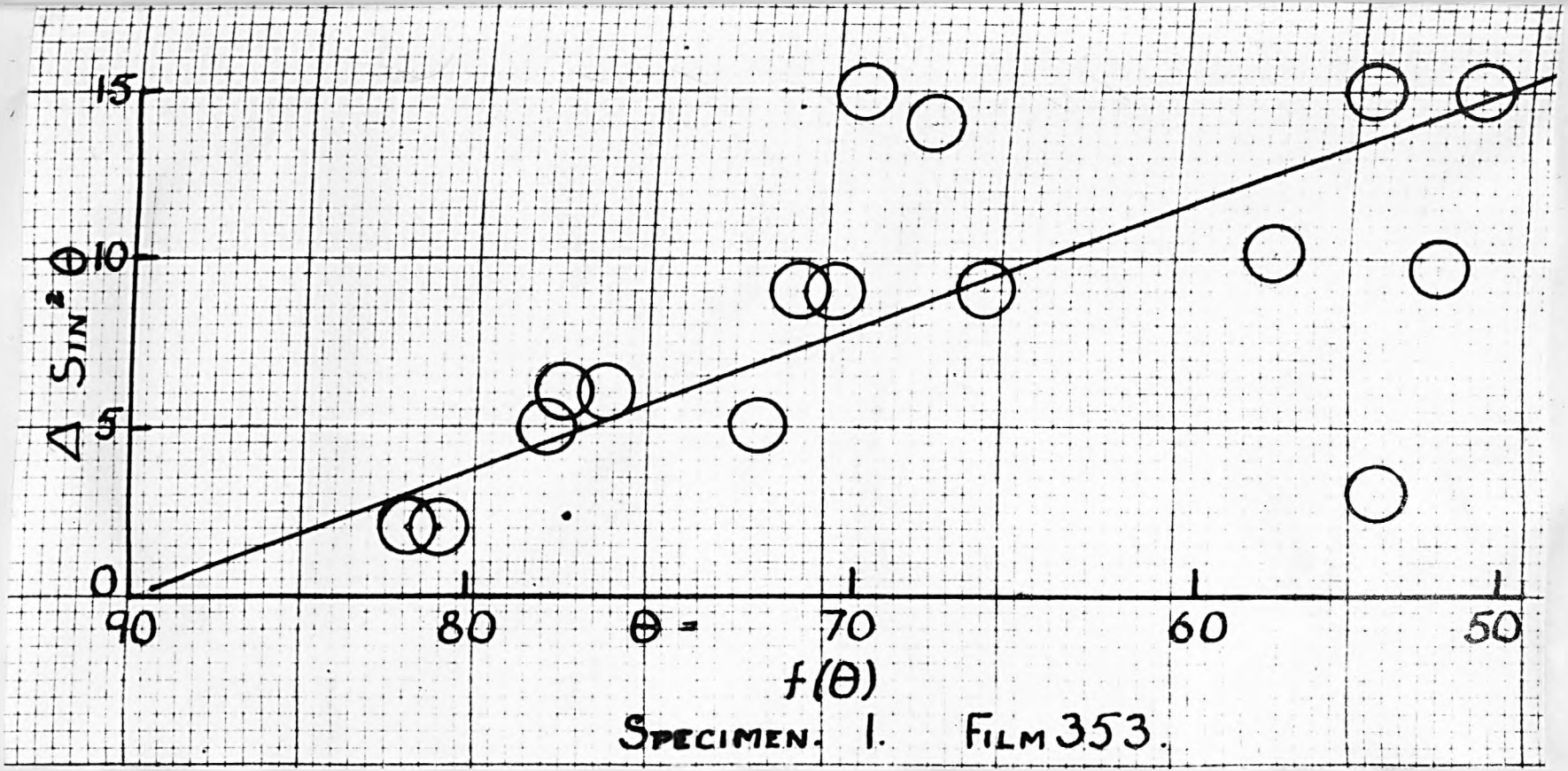

Figure 8 (a).

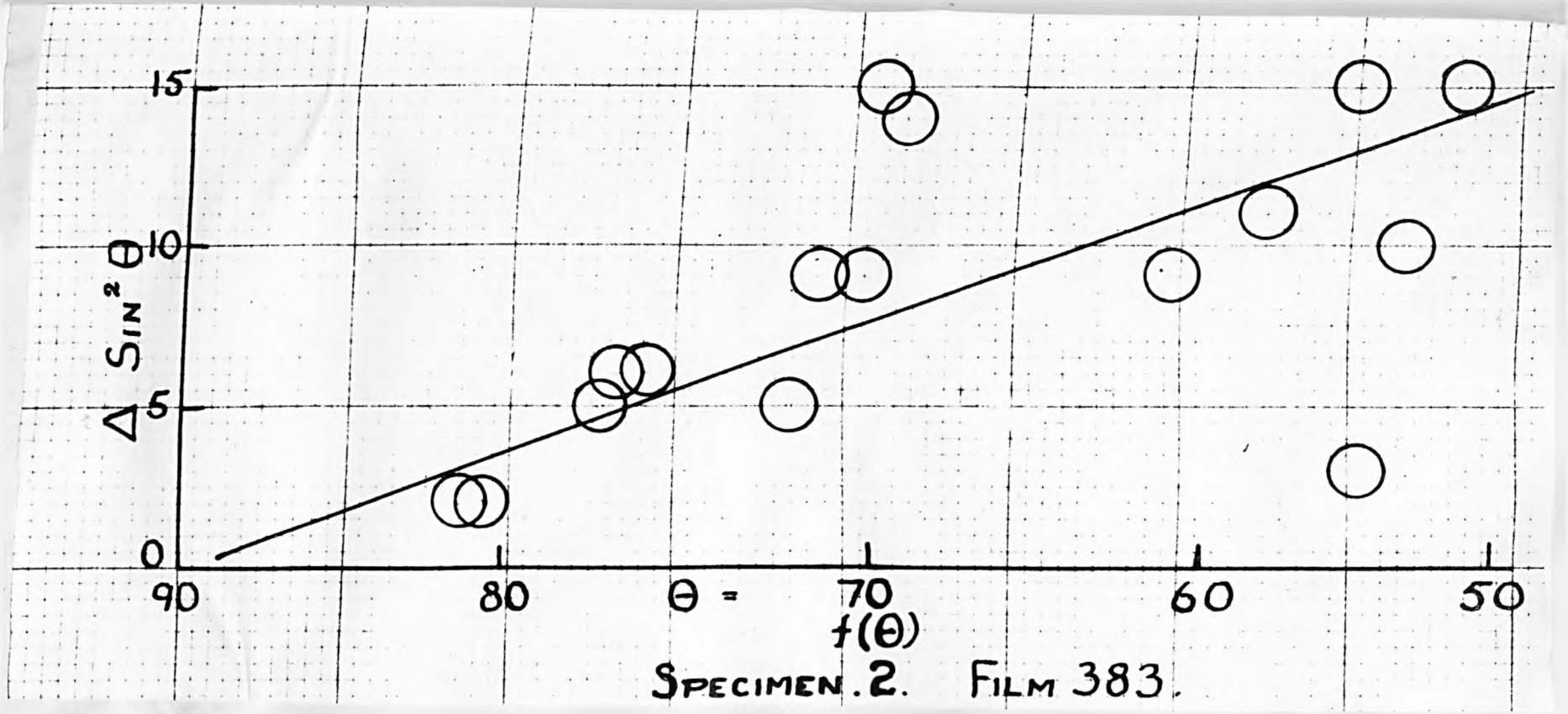

Figure 8 (b)

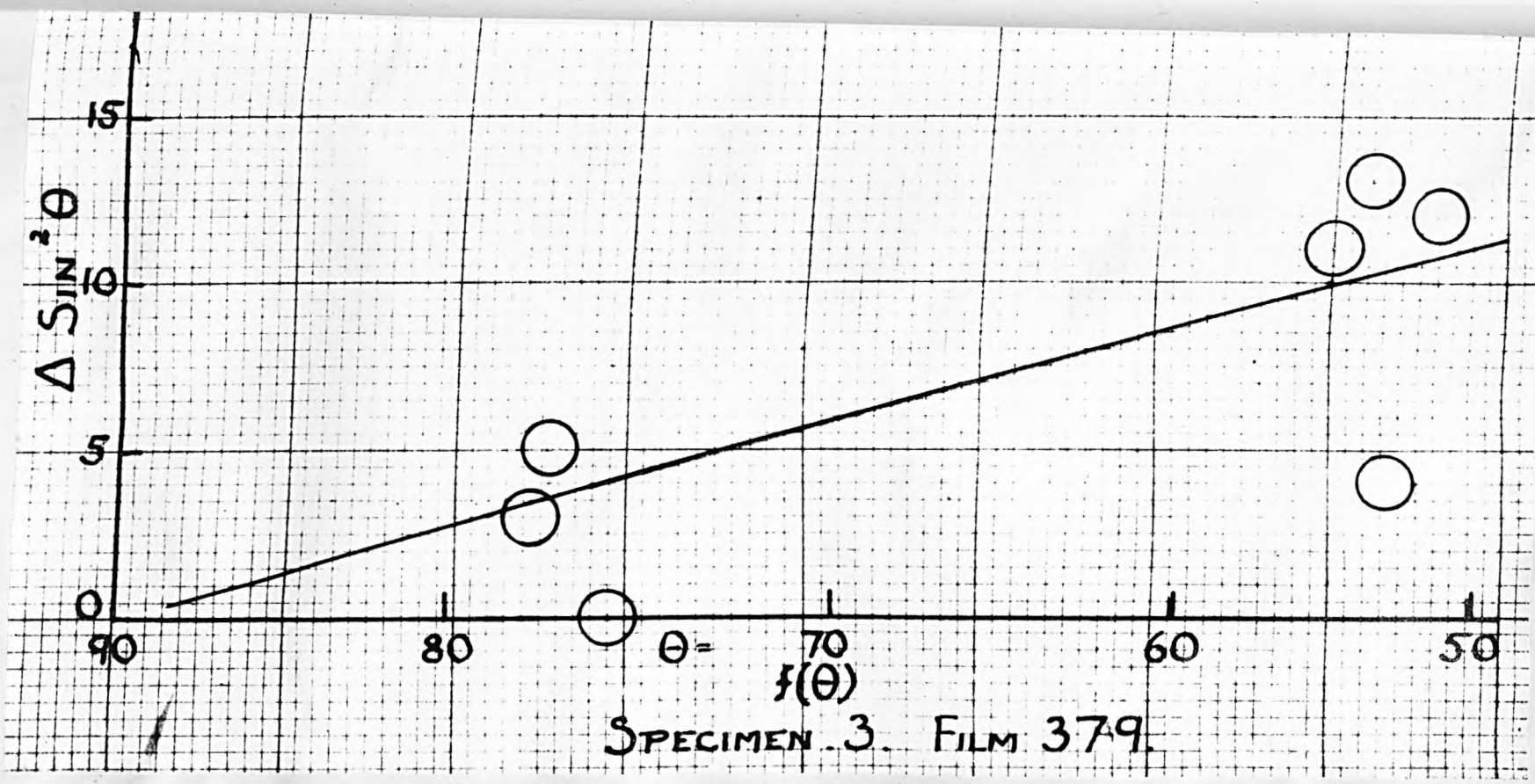

Figure 8 (c)

ratio. These lines, however, do not provide so sensitive a test for a/b as the values of h are similar; but the overlap 423. 145 contains lines with sufficiently different values of h to be used as a test for this ratio. These two overlaps on films 1 and 2 were examined visually and on a Hilger microphotometer. The overlap 136 α_1, 251 α_2 showed a curve with a flat top about 0·1 mm. wide and the lines 423.145 were seen to be an exact overlap. These results are precisely those required by the chosen axial ratios and are the same as those found by Hume-Rothery, Raynor and Little when investigating the cementite structure.

The diffraction lines from the carbide were very sharp and it was therefore expected that it would be possible to measure the parameter of the ferrite structure accurately and thus enable an estimate of the silicon content to be made. The specimens were too hard to powder by any means other than crushing and, for reasons which have already been explained, suitable diffraction patterns cannot be obtained from X-ray samples prepared in this manner. The back reflection focusing camera was set up to give

a sharp diffraction pattern when a microspecimen of annealed pure iron was used as the specimen (see Appendix 1) and then used in this position to obtain patterns from each of the etched specimens 1 to 3 in turn. To ensure that the apparatus had not been disturbed the annealed pure iron specimen was exposed both at the start and finish of the series. It gave sharp lines with a well separated ~~310~~ 220 doublet on each occasion. The annealed hyper-eutectoid steel, gave sharp lines from a structure which was easily shown to be normal ferrite. The two iron-carbon-silicon alloys gave broad lines. These were identified as lines from a ferrite structure of somewhat different unit cell size than that of pure iron, but the lines were too broad to allow a determination of the parameter to be made. The fact that the ~~310~~ 220 α-doublet was not resolved gives some idea of the extent of the broadening. It thus appears that the strain produced by the somewhat rapid cooling is considerable and judging by the extent of the line broadening it is probable that the ferrite is plastically deformed. When the carbide is extracted any elastic strain which may

be present will be relieved. The sharp lines obtained from the carbides show that they do not suffer any plastic strain.

Carbide structures have a high resistance to deformation and it is not surprising that the stress is concentrated in the ferrite. This conclusion confirms the earlier view of Schwartz, Van Horn and Junge[10].

D I S C U S S I O N

As the accurate methods employed in this investigation have failed to detect any change in the unit cell dimensions of cementite when silicon is introduced into iron-carbon alloys it is concluded that the solubility of silicon in the carbide phase is negligible.

The determinations in the present investigation were all carried out at 20°C. Petch[22] investigating the variation of carbon content of cementite from iron-carbon alloys was unable to detect any deviation from the 3 Fe: 1 C ratio at temperatures below 680°C, but did find a small residual variation in the unit cell dimensions at higher temperatures; any changes

in carbon content accompanying these variations were too small to be detected by chemical analysis. He suggested that the variation is produced by carbon atoms leaving the interstices of the lattice. The atomic size of silicon does not permit this type of solution and no analogy can be drawn. However, cases are frequently encountered where the solubility of an element in a substitution type of solution increases with increasing temperature, but it does not appear to be likely in this case as the specimens examined were cooled at very different rates. If appreciable solubility existed at higher temperatures it would be expected that some variation would be found at least in specimen 3 which was quenched rapidly.

THE IRON-CARBON-SILICON EQUILIBRIUM DIAGRAM

Although Petch's work suggests the possibility of a very small variation in the composition of the carbide phase in iron-carbon-silicon alloys at high temperatures, such variation would be too small to be of importance in the following argument wherein it is assumed that the phase is of fixed composition corresponding to the formula Fe_3C. If the conventional

view of the iron-carbon-silicon system is adopted, (namely a stable system, iron-graphite-silicon, represented by an equilibrium diagram of the general form described by Scheil[43], together with a metastable system, iron-carbide-silicon, represented by a diagram of the same form, superimposed upon, but slightly displaced with respect to it), then the above conclusion necessitates considerable modification in the values generally attributed to certain crucial points in that diagram.

Certain alloys in the iron corner of the iron-carbon-silicon system undergo a ternary peritecto-eutectic reaction on cooling, and thus the equilibrium diagram contains a quadrilateral plane of constant temperature representing the four-phase equilibrium between the melt L, α -iron solid solution containing carbon and silicon (the point α), γ -iron solid solution containing carbon and silicon (the point γ) and either graphite, in the stable system, or carbide, in the metastable system. This four-phase plane is shown on a basal projection in figure 9. The quadrilateral is defined by the four points representing the compositions of the four phases taking part in the reaction and as the

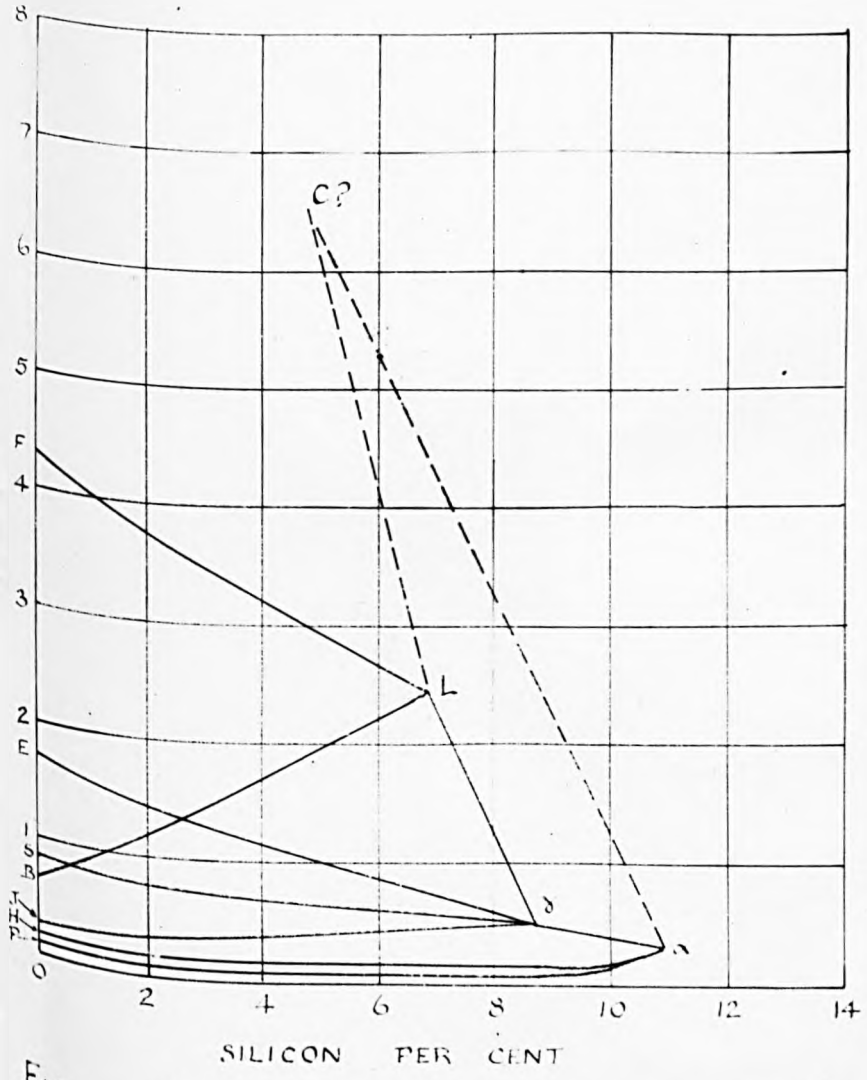

FIG. BASAL PROJECTION FE-C-SI DIAGRAM (METASTABLE)

Figure. 9.

reaction is invariant their compositions are fixed. Neither the carbide phase in the metastable system, nor the graphite phase in the stable system contain silicon[48] and thus the point C must be placed at 6·69% carbon and 100% carbon respectively. The points α and γ have been arrived at by a number of different methods with fairly good agreement between the results[49.46.45.] They probably lie close to the values:

	Metastable		Stable	
	Silicon	Carbon	Silicon	Carbon
α	11%	0·3%	10·5%	0·25%
γ	8·7%	0·5%	7·2%	0·4%

The point L is determined by the intersection of the binary peritectic line B L (figure 9) and the binary eutectic line FL. The path of the eutectic line has been extensively investigated[40.45.50.51.52.53] and the agreement is surprisingly good in view of the wide variation in the purity of the materials used. The path of the peritectic line has been the subject of only one investigation[45] and only three experimental points (including the peritectic point of the iron-carbon system) are shown on the curve. The difficulty

of establishing equilibrium conditions when cooling a ternary alloy through a binary peritectic is well known and in view of the rather rapid rates employed by Kříž and Poboril it is unlikely that these points are very accurate. Other determinations of the L point have depended upon the detection of a small change in direction of the eutectic curve which is supposed to occur at this point. The most reliable experimental values to date for the position of the L point[45] are probably

	Silicon	Carbon
Metastable	6·9%	2·61%
Stable	6.4%	2·54%

It may be shown from the general theory of equilibrium diagrams that, for a reaction of the type under consideration, the points C, α, γ and L must lie at the corners of a quadrilateral which cannot contain a re-entrant angle. For the stable system this condition is satisfied if the values detailed above are adopted. However, in the case of the metastable system these values produce a re-entrant angle at L (figure 10). There are two possible ways in which this discrepancy

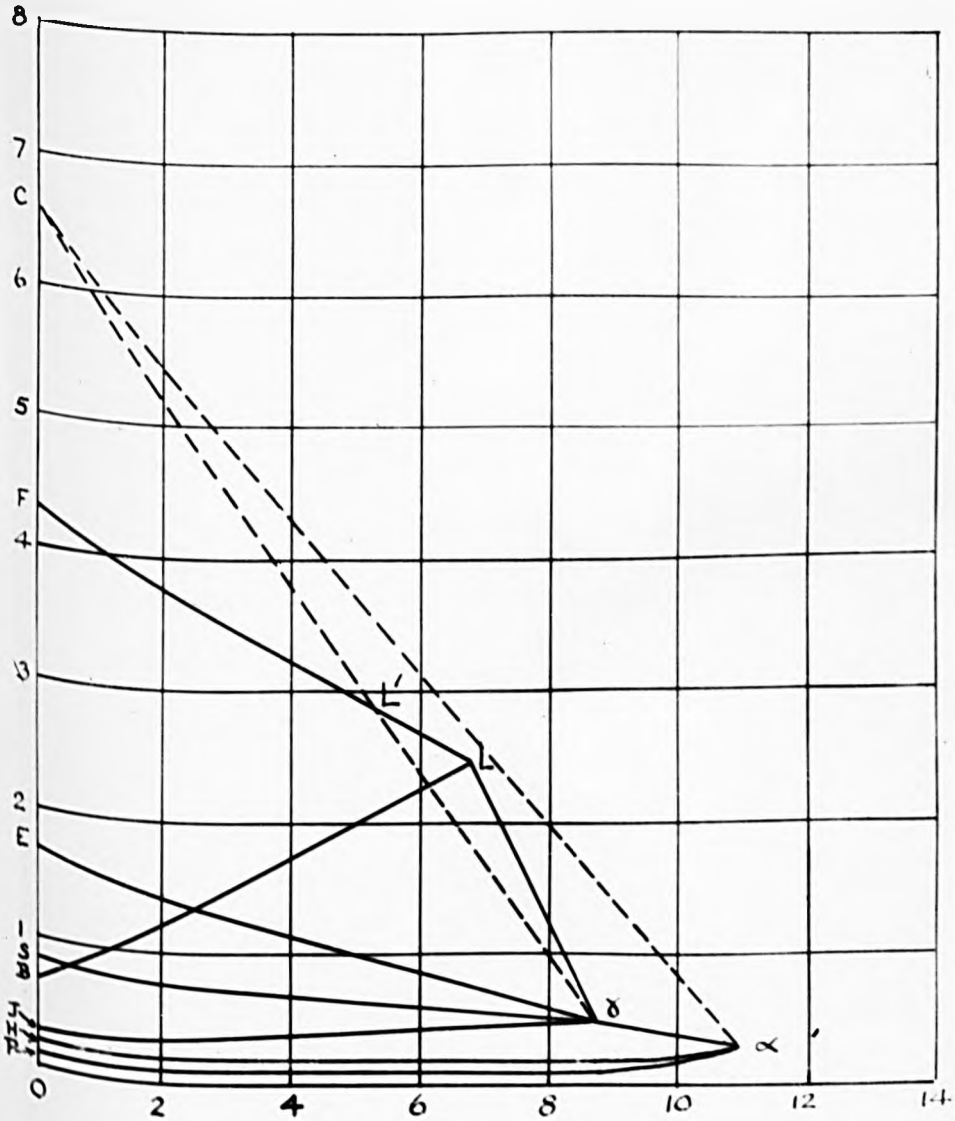

FIG. A POSSIBLE POSITION OF THE FOUR-PHASE PLANE

Figure. 10.

could be accounted for. There may be an appreciable error in the experimental values for the points in the metastable system. If this is the case, it appears most probable, for reasons which have been indicated earlier, that the greatest error is in the position of the point L. If it is assumed that the path of the binary eutectic, as shown in figure 10, is approximately correct, the maximum possible silicon content at the point L appears to be about 5% with a corresponding carbon content of about 2·9% (point L' figure 10). Alternatively, this difficulty would not arise if the view were adopted that the theoretical rules applicable to equilibrium diagrams are invalid when applied to metastable systems. The published data for the metastable part of the double diagram could be considered merely as a representation of the conditions existing when rather impure alloys are cooled in such a manner that appreciable undercooling is produced.

It is clear that a new experimental determination of the point in both the metastable and stable systems is necessary. We are now carrying out this

work at Liverpool, using high purity materials melted in vacuo.

THE INFLUENCES OF MANGANESE, SULPHUR AND PHOSPHORUS ON THE CARBIDE IN IRON-CARBON-SILICON ALLOYS.

I N T R O D U C T I O N

It is well established from industrial practice that the stability of the carbide in cast irons is influenced to a pronounced degree by the amounts of manganese, sulphur and phosphorus present. Although extensive accounts exist of the relation between composition and carbide stability in iron of commercial quality, no published work has appeared concerning the influence of these elements when added separately to high purity iron-carbon-silicon alloys. In the work to be described an attempt was made to determine the effects of separate additions on the structure and composition of the carbide.

The compositions of the various alloys chosen for investigation were dictated by a number of factors:

The alloys had to solidify in the metastable system under the conditions of cooling employed, i.e. graphitisation had to be prevented. The cooling rate was already fixed by the nature of the experimental arrangement used for melting and cooling the alloys; an arrangement which has enabled carbide to form in

high purity alloys of reasonably high carbon and silicon content, without producing such internal stress conditions as to broaden the X-ray diffraction lines. It was also considered desirable that the carbon and silicon contents should be of the same order of magnitude as those employed in the earlier work and, finally, that the amount of addition element should be as large as possible to produce the maximum effect, without being sufficient to cause the appearance of crystal structures which do not occur in commercial irons.

THE EFFECT OF MANGANESE

The crystal structure of the carbide phases in iron-carbon-silicon-manganese alloys have not been previously reported. As long ago as 1910 it was shown, by chemical methods, that the carbide constituent in ternary iron-carbon-manganese alloys contains appreciable amounts of manganese. In 1933 Jacobson and Westgren showed that the manganese carbide Mn_3C is isomorphous with cementite (Fe_3C) and completely intersoluble with it. Since that time all the ternary equilibrium diagrams have shown the carbide phase as having a continuous range of

composition between these two intermediate constituents. The general form of the diagram at room temperature (taken from a paper by Goldschmidt[66]) is shown in figure 11. Unfortunately, no experimental determination of the ternary system in the composition range in which we are interested (namely, 2·5% carbon, 2.0 - 4·5% manganese) has been made, the nearest approach being in the work of Gensamer[67] who investigated a constant manganese section, at 4·5% manganese, up to 1·3% carbon. The vertical section which he produced is shown in figure 11a. In the discussion of their earlier work, Bain, Davenport and Waring[68] remarked that, "The impoverishment of the ferrite, with respect to its manganese, by carbide formation raises the critical temperature (of the eutectoid) sharply" and thus the sharp rise of both the eutectoid lines in the vertical section indicates that the manganese content of the carbide increases with increase in carbon content. This argument leads to the conclusion that the manganese content of the carbide is considerably greater than the average manganese content of the alloy. Estimates of the proportions of manganese present in the carbide, made

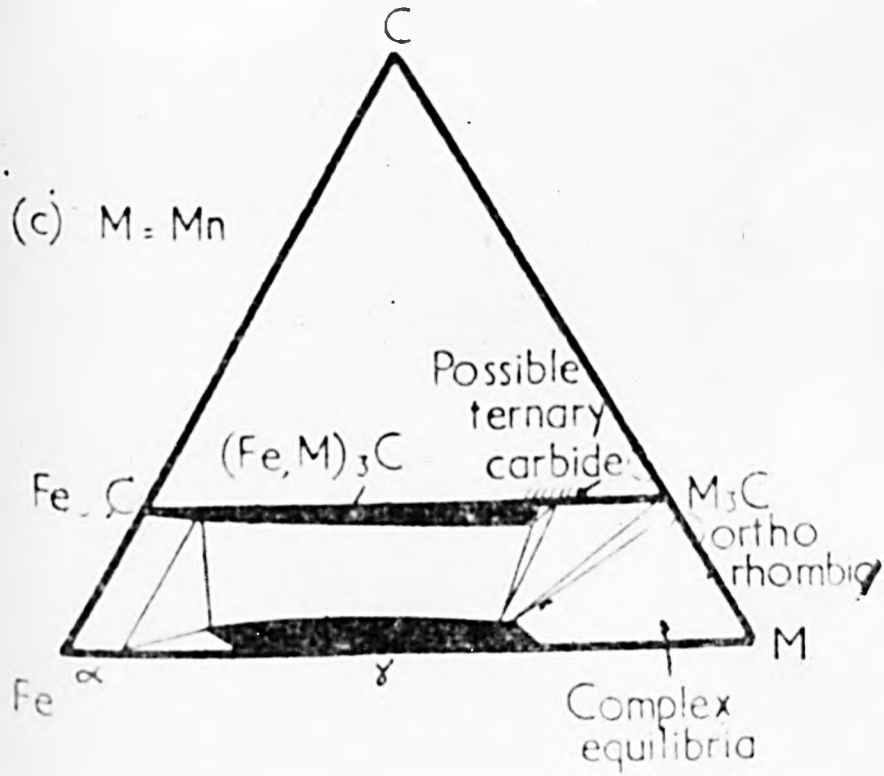

Figure 11. General Form of the Iron-Carbon-Manganese Diagram.

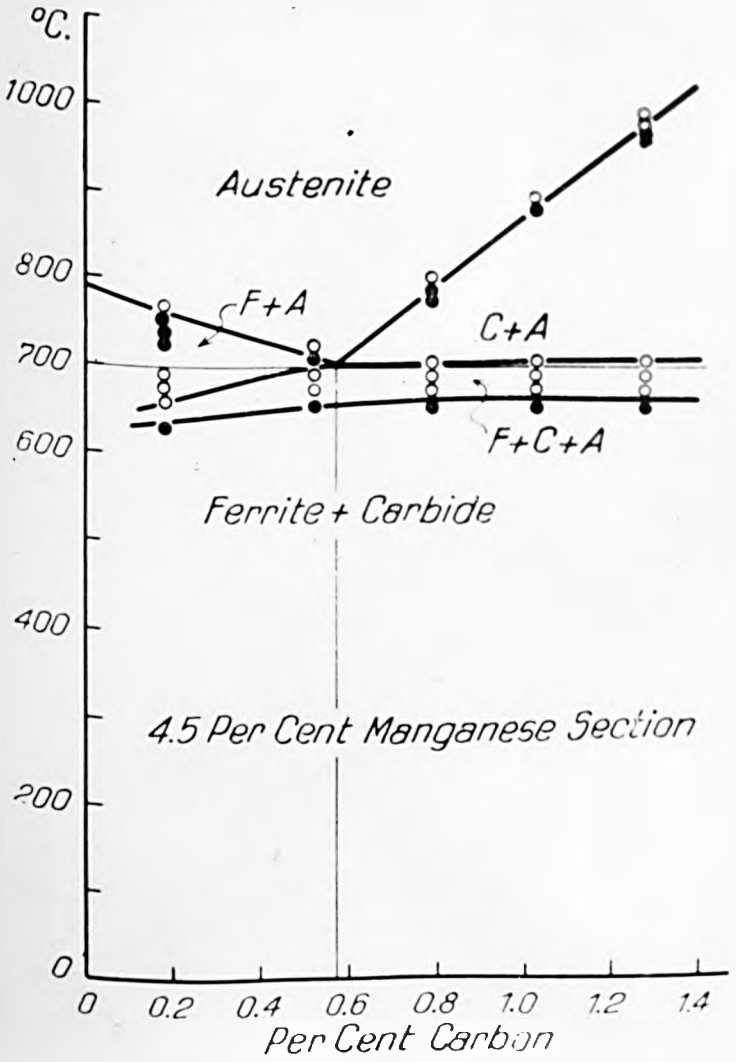

Fig. 2—4.5 Per Cent Manganese Section of the Constitution Diagram for the Ternary System Iron-Manganese-Carbon.

Figure 11a.

by deduction from experimental studies of the equilibrium diagram, have usually indicated a very high manganese content[68,69,70]. By chemical analysis, Arnold and Reed[64] found the manganese content of the carbide, in an alloy containing 7% manganese to be about 20%. On the other hand, several of the ternary diagram isothermal sections at low temperatures show a two-phase field, α + carbide, in which the carbide contain less than this, Vogel and Doring[69] label this same field α + Fe_3C, although it is clear from a consideration of its position that the carbide contains at least a small percentage of manganese. The matter may be summarised by saying that it is well established that the iron atoms in the cementite structure may readily be replaced by manganese atoms, although the extent to which it happens in the ternary alloys is not clear; the most reliable information suggests that the manganese content of the carbide is high and may be as much as 20% in the higher manganese alloys. There is no evidence to suggest the effect of silicon on this manganese content.

E X P E R I M E N T A L

The manganese used in this investigation was high purity distilled manganese supplied by Johnson Matthey and Co. Ltd., the other basic materials being the same as those used in the previous work.

Due to the ease with which manganese volatalises, the alloys could not be melted in vacuo. The melting of high purity iron alloys containing manganese has been discussed in detail by Gayler[71] and Walters[72]. Their recommendations have been adopted in the present work wherever they are applicable. Deoxidation treatment with hydrogen was not necessary as the alloys contained large amounts of carbon.

The recrystallised alumina crucible holding the charge (50 gms) was supported in a vertical tube furnace by an alumina cylinder, (see figure 12). A Mullite tube, surrounding the crucible and separating it from the outer silica tube, was cemented to this cylinder so as to form a receptacle for the molten metal should the crucible break during a run. A brass cap, containing an observation window and inlet pipe for the argon, was sealed to the top of the outer silica tube. The tube was closed at the bottom by a

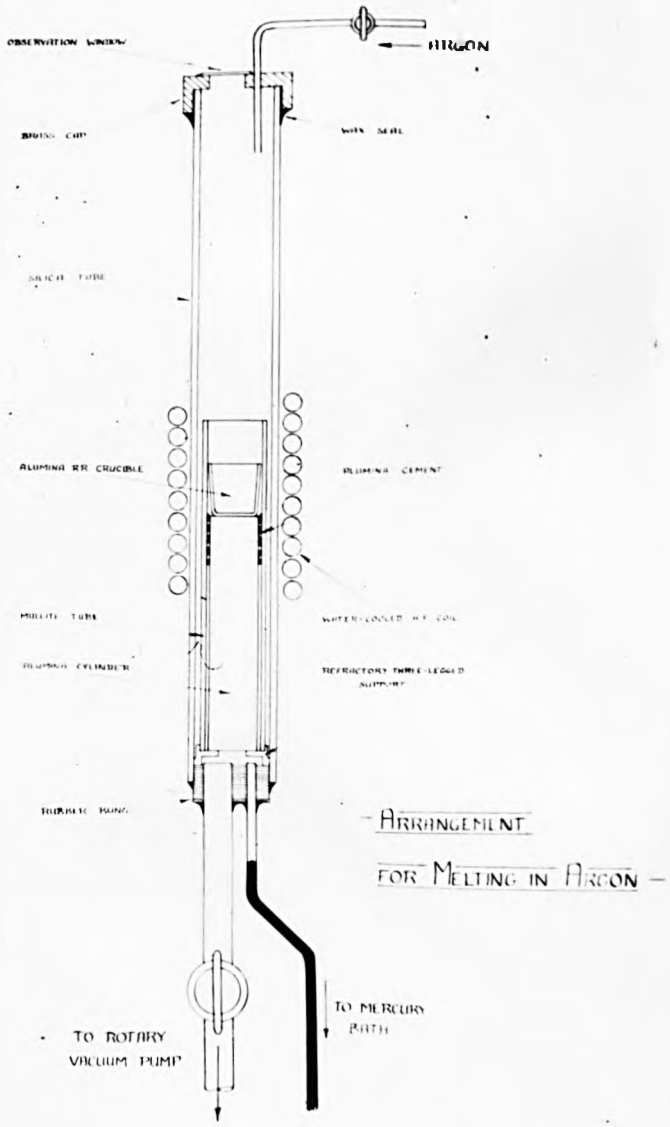

- ARRANGEMENT FOR MELTING IN ARGON -

Figur e. 12.

wax sealed rubber bung through which was passed an half inch diameter pipe leading to a rotary vacuum pump, and a smaller diameter pipe dipping into a mercury bath three feet beneath. A three legged refractory support was used to lift the alumina cylinder clear of the inlet to the vacuum tube. The charge was heated by means of a water cooled high-frequency coil.

After closing the gas inlet tap, the apparatus was pumped out until a vacuum of about 0·1 mm. mercury was obtained. The gas inlet tap was then opened and the vacuum tap closed. The pressure of the argon was increased until it was sufficient to ~~course~~ cause the gas to bubble slowly through the mercury bath, thus ensuring a positive pressure of about 1" mercury above atmospheric. This positive pressure was maintained throughout the melting and cooling cycle. This method of filling the tube was adopted as it is more satisfactory and less expensive than the, more usual, method of sweeping the air out with the argon. When the gas had been flowing for a few minutes the coil was energised and the charge melted as rapidly as possible. After a few minutes superheating treatment the current was switched off and the alloy allowed to solidify in the crucible.

The first four melts that were made contained about

3% carbon, 3·5% silicon and between 4% and 8% manganese, but did not solidify white. After further trials three ingots were obtained which were white except for a very small graphitised volume at the centre. This graphite was of the Type D variety. [redacted]. Microscopic examination of the earlier grey ingots showed the graphite to be present as large flakes. This experience indicates that manganese in high purity alloys is not so strong a carbide stabiliser as was to be expected from observations on commercial alloys. On analysis the three white ingots were found to contain:

	Carbon	Silicon	Manganese	Film
Ingot M.1	2·48%	2·81%	1·73%	421
Ingot M.2	2·43%	3·13%	3·24%	423
Ingot M.3	3·41%	3·15%	3·37%	429

The manganese figures are an average of three results, the variation being much greater than could be accounted for by possible error in the analysis. Each ingot was sectioned and examined microscopically. All the alloys were very clean and on etching showed massive carbide embedded in a pearlitic matrix, see figures 13,

14 and 15. Considerable variation in the size and distribution of the carbide and pearlite areas was noticed. This heterogeneity probably accounts for the variation in the analysis results. It has been noted on a number of previous occasions that it is unusually difficult to obtain uniform manganese distribution in alloys melted under similar conditions. For example, Gensamer found that it was necessary to subject an alloy, containing 1·3% carbon and 4·5% manganese. to a severe forging treatment followed by 12 hours annealing at 1095°C in order to obtain a homogeneous ingot. Such treatments are not possible with the present alloys as they will not forge and annealing treatments at temperatures above 700°C cause decomposition of the carbide.

Two films of each sample were obtained and all the films were measured on a travelling vernier microscope and compared visually with the films of cementite in iron-carbon and high purity iron-carbon-silicon alloys. The lines were not as clear as those obtained from the high purity ternary alloys and all the lines appeared slightly broadened. To discover whether or not this difference was due to any difference

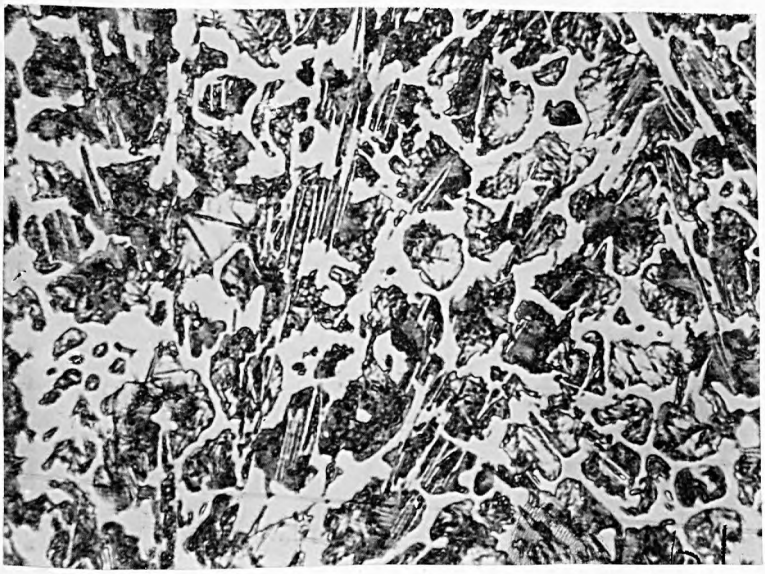

Figure. 13. Carbide in Fe-C-Si Alloy containing Manganese. Specimen M1. x350.

Figure. 14. Carbide in Fe-C-Si Alloy containing Manganese. Specimen M2. x350.

Figure, 15. Carbide in Fe-C-Si Alloy containing Manganese. Specimen M3. x350.

there may have been in the focusing of the tube or alignment of the cameras another series of samples were exposed, the samples containing manganese being interspersed with the samples which had previously been used in the work on the iron-carbon-silicon alloys. All the samples from the previous investigation gave sharp lines which were identical with those which had been obtained previously, whilst the alloys containing manganese gave slightly broadened lines; demonstrating that the results were characteristic of the specimens. On visual examination, the patterns appeared to be the same as those obtained from cementite. All the lines which had previously been recorded from this structure were visible with the exception of seven weak high angle lines which included 432 α_1, 432 α_2 and 046. There did not appear to be any difference between the spacing of the lines and that of corresponding lines on films from cementite, although it was difficult to be certain on this point as the lines on films M1, M2 and M3 were a little broader. Seven distinct lines ranging in θ values from 48° to 78° were measured and the difference between these experimental values of $\sin^2\theta$ and the values calculated

from the parameters of cementite were plotted against $\left[\sin 2\theta + \sin^2\theta \left(\frac{\cos^2\theta}{\sin\theta} + \frac{\cos^2\theta}{\theta}\right)\right.$ The curves were extrapolated to $\theta = 90^\circ$. The results are set out in Table 2, appendix 3, and the curves are shown in figure 16a,b,c. As the lines could not be measured with the same accuracy as had previously been achieved the points show considerable scatter. However, it is clear that in each case there is a small residual difference in the values of $\sin^2\theta$, being about ·0008 on film M1, and 0010 on films M2 and M3. These differences are little larger than the estimated experimental accuracy, as can be seen by considering the scatter of the points in figure 16a. However, as they represent a mean through a number of results, it is considered that the existence of a small difference has been established with certainty. The 136 α_1, 251 α_2 overlap was broadened; however, it cannot be determined whether this broadening is due to the same cause as that of the general broadening found on all the lines or is due to a change in the extent of the overlap.

An idea of the magnitude of the change in cell size necessary to produce the differences in $\sin^2\theta$ discussed above may be obtained by considering, say,

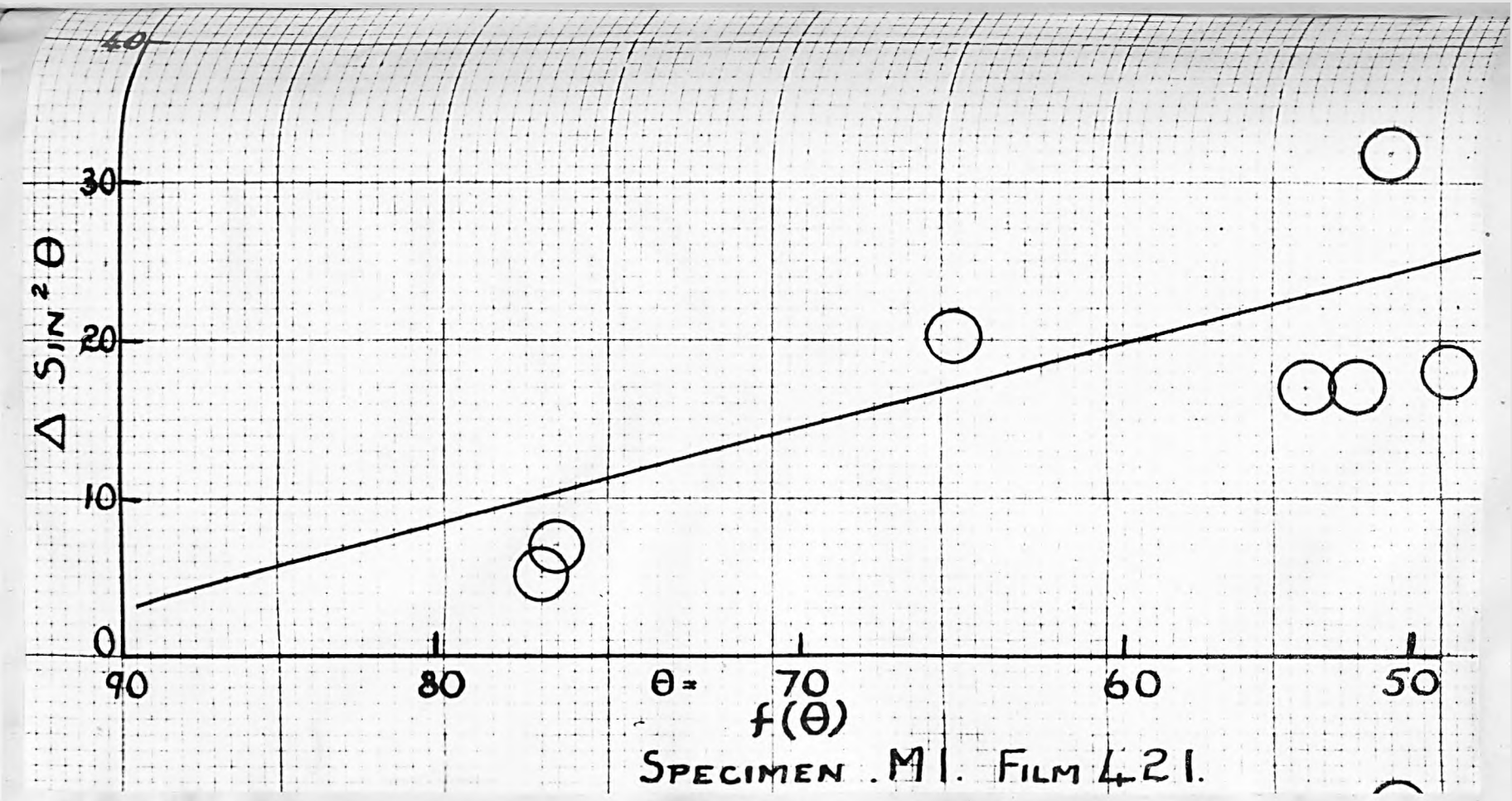

Figure 16 (a)

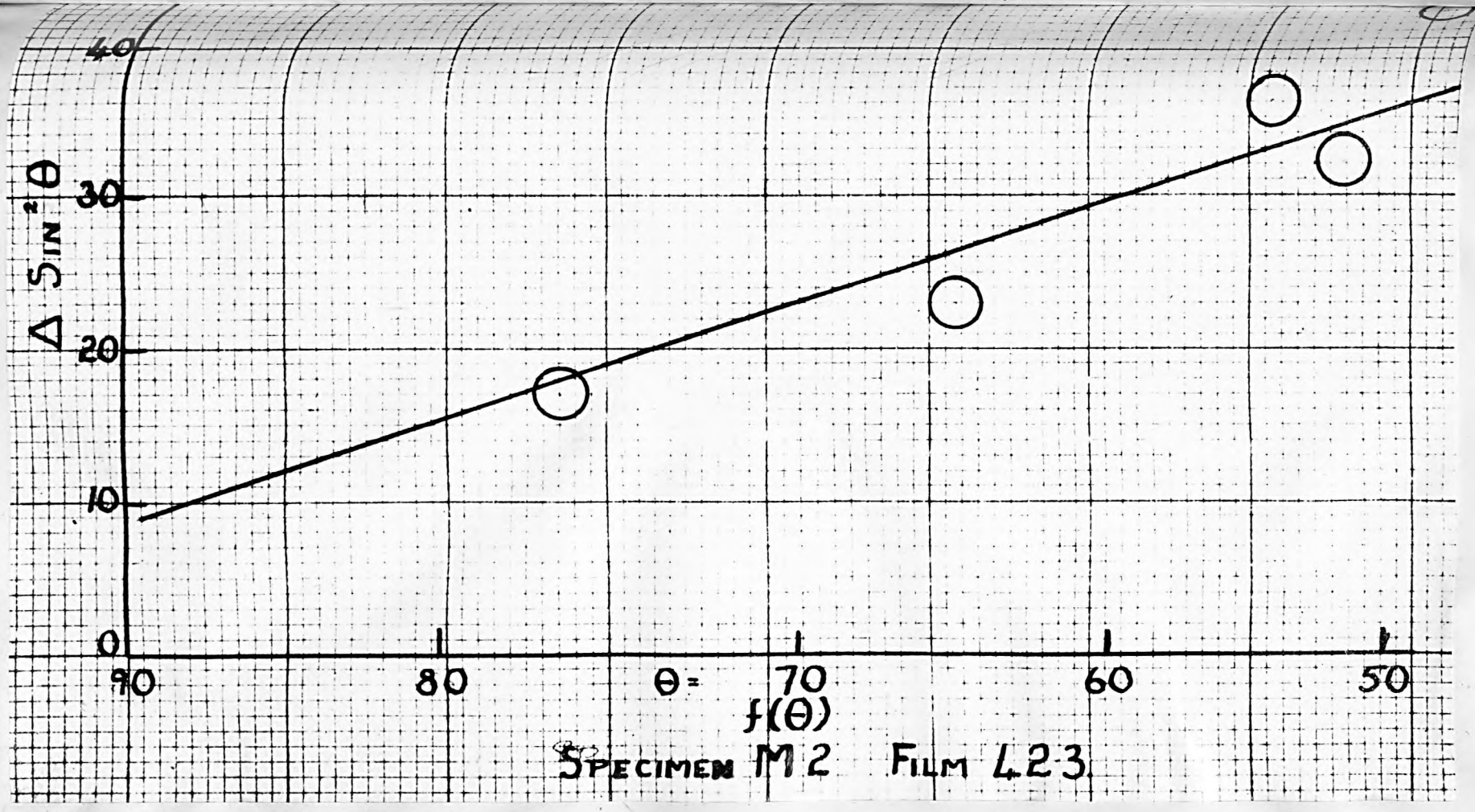

Figure 16 (b)

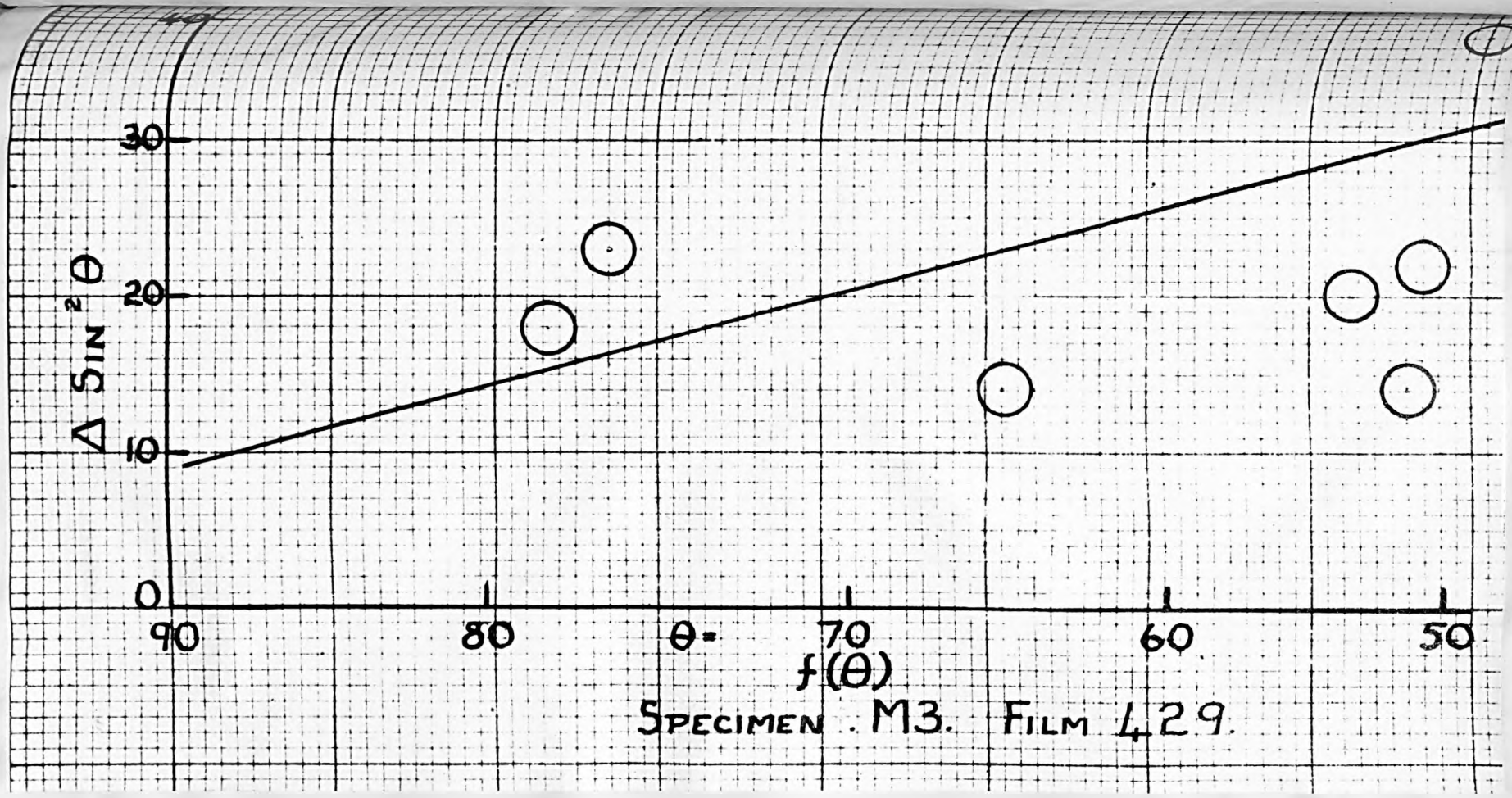

Figure 16 (c)

the highest angle line of film M3, namely 136 α_2. From the curve in figure 16a it appears that the difference in $\sin^2\theta$ for this line is about 0·0017, and if it is assumed that each of the cell sides of the orthorhombic cell decrease by the same amount, this would correspond to a contraction of about 0·0006 Å.

DISCUSSION OF RESULTS.

It is concluded, from the above results, that the carbide in iron-carbon-silicon alloys containing up to 3·4% manganese is cementite. The parameters of the unit cell are only very slightly different from those of cementite in plain carbon steels or high purity iron-carbon silicon alloys. This small difference in cell size suggests that a very small amount of manganese enters the structure.

It has been demonstrated that the line broadening is not a result of the experimental conditions. As no line broadening due to plastic deformation was detected in the carbides extracted from iron-carbon-silicon alloys cooled under similar conditions, or on the films of extracts of these alloys containing sulphur and phosphorus which were cooled under identical conditions (see later), it seems unlikely

that the broadening is due to this cause. The only possible explanation appears to be that the broadening is due to a variation in the composition of the carbide, and heterogeneity of the ingot has already been demonstrated; as the carbide in alloys which do not contain manganese is of fixed composition, the variation can only be accounted for if it is assumed that the structure contains some manganese atoms.

The bonding of the cementite structure has been discussed in an earlier chapter, when it was mentioned that the iron-iron bond distance was of the same order of magnitude as that found in ferrite or austenite and that each iron atom has 11 or 12 close neighbours. These bond distances are within the range 2·48 to 2·68 Å. The manganese atoms which have 12 neighbours in the α-manganese structure have a bond distance of 2·71 Å. From this it appears that manganese has a favourable size-factor for replacement of iron atoms in the cementite structure and, as the difference in atomic size is not very great, it might be expected that the rate of increase in the size of the cell with increase in manganese content would be small. Unfortunately, no figures for the change of cell size with manganese content are available. The results of

the present investigation indicate a decrease, rather than an increase, in cell size and thus it is clear that no estimate of the manganese content can be made by applying Vegard's law using the values of atomic sizes mentioned above. It is well established that chromium, which also has a favourable size factor, and a somewhat larger atomic size than iron, produces a large decrease in the unit cell size of cementite when it enters the structure in small amounts[21]. Thus, it is not possible to estimate the percentage of manganese present in the carbides examined in the present investigation. However, as the change in lattice parameter which is produced is very small indeed it is concluded that the percentage of manganese is very small and certainly very much less than the 10 to 20% that is estimated to be present in iron-carbon-manganese alloys containing about 4% manganese. This result, which may at first sight appear surprising, is not unreasonable when it is realised that an element which has a favourable size-factor to enter the cementite structure will also have a favourable size factor to enter the austenite and ferrite structures. The free-energy values of the constituents will determine the distribution of the

manganese addition. Thus, it appears that the addition of silicon to an iron-carbon-manganese alloy causes a redistribution of the relative free-energies of the constituents such that the manganese enters the austenite and ferrite structures in preference to the cementite structure. This matter is considered in greater detail in the general discussion.

THE EFFECT OF SULPHUR.

Several experimental investigations have been made of the iron-carbon-sulphur system.[73.74.75.] No carbides, other than cementite have been found. There is no evidence to suggest whether or not sulphur enters the carbide, although it appears to be generally supposed that it does not. The influence of silicon on these alloys has not been reported.

EXPERIMENTAL

The introduction of controlled amounts of sulphur into high purity iron-carbon-silicon alloys presented some difficulty. It was eventually decided to prepare an alloy by satuating the melt with sulphur. This was carried out in the same apparatus as that used for melting the alloys containing manganese. (The apparatus was first cleaned thoroughly to remove all

traces of manganese). Ten grams of analytically pure sulphur was wrapped in a thin sheet made of high purity iron and embedded in the charge (50 grms) which was composed of the same basic high purity materials as were used in the previous experiments. The heating and melting cycle was carried out in exactly the same manner as that described for the preparation of the alloys containing manganese. Just before the alloy was molten the argon bubbling through the mercury trap was seen to be saturated with condensed sulphur vapour. The amount of sulphur present was sufficient to saturate the argon throughout the whole run.

On microscopic examination of the sectioned ingot the alloy was seen to be clean except for the presence of large globules of the microconstituent which is generally recognised as iron sulphide (Fe S). The carbide was of the normal massive variety and was surrounded by pearlite. The iron sulphide globules can be seen on the microphotograph reproduced in figure 17. On analysis the alloy was found to contain:

	Carbon	Silicon	Sulphur	Film
Ingot 31.	2·09%	2·00%	1·66%	425.

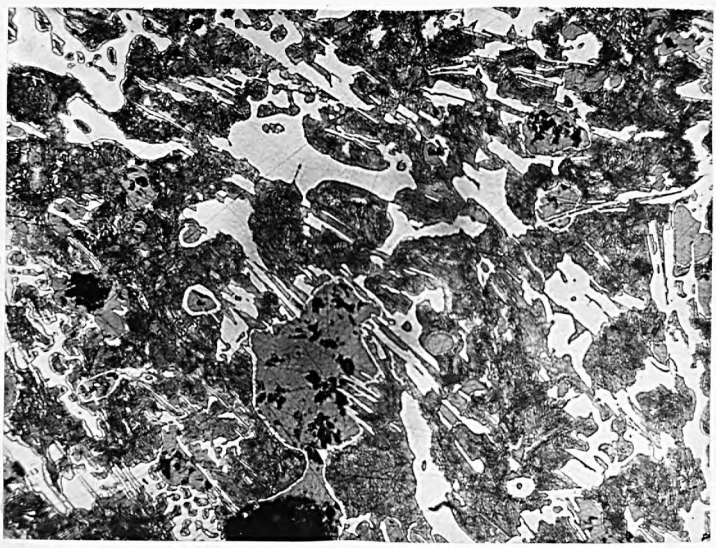

Figure. 17. Carbide in Fe-C-Si Alloy containing Sulphur. Specimen S1. x350.

Three X-ray films were obtained of the extracted carbide. On all of these the lines were sharp and the pattern was the same as that obtained from cementite. By visual comparison the line spacing appeared to be identical with that on the cementite films. The films were measured on the travelling vernier microscope and the values of $\sin^2\theta$ calculated for each line, when it was found that all the lines could be indexed with certainty on the basis of the cementite structure. The difference between the experimental values of $\sin^2\theta$ for the cementite structure and those calculated for nine strong high angle lines were plotted against $\left[\sin 2\theta + \sin^2\theta\left(\frac{\cos^2\theta}{\sin\theta} + \frac{\cos^2\theta}{\theta}\right)\right]$ when it was found that the difference disappeared when θ approached 90^0 (Table 3, Appendix 3). The 136 α_1, 251 α_2 and 423. 145 overlaps were examined and found to be the same as those on the cementite films.

DISCUSSION OF RESULTS.

It is concluded that the carbide in iron-carbon-silicon alloys containing sulphur is cementite (Fe_3C) and that sulphur does not enter this structure.

When sulphur forms compounds with iron the bonding between these elements is strongly electrovalent. It would not be expected, therefore, that sulphur would replace iron to any great extent in a compound in which the bonding is essentially metallic.

THE EFFECT OF PHOSPHORUS

No carbides, other than cementite, have been reported in accounts of experimental work on the ternary iron-carbon-phosphorus system,[76,77] nor is there any suggestion that phosphorus can enter the cementite structure. Künkele[77] showed that when the carbon is present as cementite in a quaternary iron-carbon-silicon-phosphorus alloy a ternary eutectic of iron-silicon-carbon-phosphorus solid solution, cementite (Fe_3C) and iron phosphide (Fe_3P) is formed which can be distinguished in the final structure by normal microscopic methods.

E X P E R I M E N T A L

An high purity iron-carbon-silicon alloy saturated with phosphorus was prepared in a similar manner to that employed to produce the high sulphur alloy, red phosphorus being packed into a small container made of high purity iron and embedded in the charge. The argon was laden with phosphorus

vapour before the charge was molten and it was necessary to ensure that sufficient was present to saturate the gas during the whole of the cycle. The first alloy prepared in this way contained 2·49% carbon 1·95% silicon and about 3·0% phosphorus and solidified grey with a flake aggregate type of graphite structure (see figure 19). As a similar alloy without phosphorus solidified white, this result was rather surprising. Phosphorus is not generally supposed to be a graphitising agent. The alloy had to be remelted and diluted with pure iron several times before a white ingot was obtained which contained 1·84% carbon, 1·67% silicon and 3·59% phosphorus. A microscopic examination of a section through this ingot showed the metal to be clean. The microstructure consisted of areas of fairly coarse pearlite surrounded by large areas of the ternary solid solution-cementite-phosphide eutectic interlaced with plates of iron phosphide (see figure 20). This alloy was treated electrolytically with dilute hydrochloric acid in the usual manner and the extract was examined by the same X-ray methods as those used in the previous work. The film obtained had 30 sharp clear lines which, however, were not of the pattern produced by the cementite structure. There were, in addition, three

Figure. 19. Graphite in Fe-C-Si Alloy containing Phosphorus. x350.

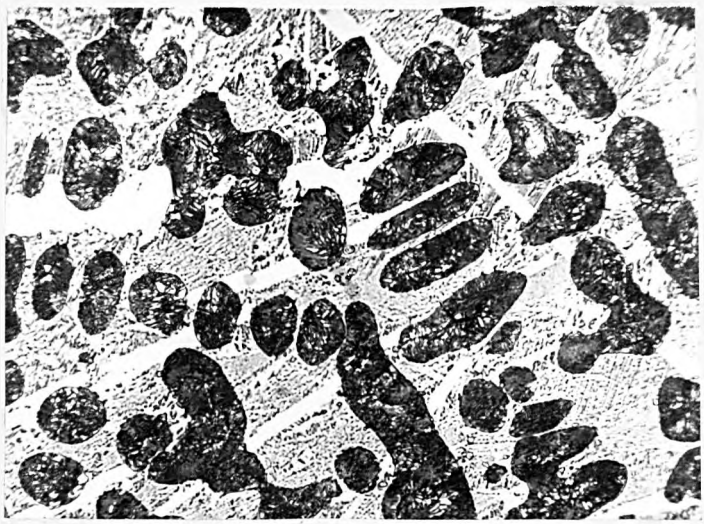

Figure. 20. Fe-C-Si Alloy containing Phosphorus.
This alloy has solidified white.
Specimen P1. x350.

very faint low angle lines belonging to this structure, but these were, of course, useless for the purpose of determining the lattice parameter. The 30 clear lines were measured and values of $\sin^2 \theta$ were calculated. It was found that all could be indexed with certainty on the basis of the tetragonal structure of iron phosphide (Fe_3P). Calculated values of $\sin^2 \theta$ for the permitted reflections from this structure are listed in table 2, appendix 2 and the experimental values and indices of the lines are shown in table 4, appendix 3. It is evident that the extract consisted very largely of iron phosphide. In the hope that the phosphide would be attacked preferentially, the powder was treated with a boiling solution of concentracted hydrochloric acid. After 10 minutes treatment some powder remained which was washed and dried. The diffraction pattern obtained from this consisted of four very faint very broad lines of the cementite structure. Thus it seems that the carbide, which as a constituent of the ternary eutectoid is in the form of small globules, has been reduced to a very fine powder by the further acid treatment and hence a sharp diffraction pattern cannot be obtained. No other method of separating the carbide from this large amount of phosphide was discovered.

In order to obtain a diffraction pattern from the carbide it was necessary to prepare an alloy with a much lower phosphorus content so that the carbide would separate from the melt as a pro-eutectic constituent. An attempt to do this in the argon apparatus was not successful as the phosphorus was carried out of the system before the alloy was molten. The only alloy which could be obtained was one which had been used in some earlier work and had been prepared by melting a high phosphorus pig iron (containing 3·23% carbon, 2·08% silicon, 0·53% manganese, 0·06% sulphur and 1·72% phosphorus) with electrolytic iron and a little carbon and silicon in a silica crucible heated by a graphite sleeve in the high-frequency coil. The alloy contained 1·63% carbon, 1·13% silicon, 0·21% manganese 0·03% sulphur and 0·92% phosphorus. The metal had been cooled by pouring into a chill mould and was white with massive primary carbide. The films obtained from this alloy were re-examined and measured (eight clear high-angle lines are recorded in table 5, appendix 3). All the lines of the cementite pattern were present with the exception of eight faint high angle lines. The lines were sharp and the difference between the experimental

values of $\sin^2 \theta$ and those calculated from the parameters of the cementite structures disappeared as θ approached 90°.

In addition a good film was obtained from the extract of the high phosphorus grey iron which is mentioned above. This was also examined in detail. The difference in $\sin^2 \theta$ again disappeared when θ approached 90°. The results for this alloy are discussed later under the heading "Commercial Iron-Carbon-Silicon Alloys".

DISCUSSION OF RESULTS

It is concluded that the carbide in iron-carbon-silicon alloys containing phosphorus is normal cementite and that phosphorus does not enter this structure.

Unfortunately the alloys used in this section of the work were not of the same high purity as those used earlier, some containing small quantities of manganese and sulphur, but as the effect of these elements on the carbide has already been established it is considered that the small amounts present do not invalidate the deductions made from the results.

COMMERCIAL IRON-CARBON-SILICON ALLOYS

A total of sixteen different commercial grey irons and five different white irons were examined during the course of the investigation. In all cases, on visual examination of the films, the diffraction patterns of the carbide constituent were found to be identical with that of cementite. The films from four specimens were examined in greater detail. The composition and microstructures of these irons are given in table 2.

TABLE 2.

Specimen	Film	Description	C	Si	Mn	S	P	Microstructure
1.	61.	Low grade, high Phosphorus, grey iron.	3·23	2·08	0·53	0·06	1·72	Figures 21 and 22.
K7.	201.	High grade, low Phosphorus, inoculated grey iron.	1·20	1·60	0.82	0·12	0·15	Figure 23.
			inoculated: 80 oz/ton calcium silicide.					
D.	191.	White Cast Iron.	3·36	0·96	0·81	0·07	0·06	Figures 24 and 25.
E.	364.	White Cast Iron.	2·5	1.03	0·3	0·09	0·14	Figure 26.

Specimens 1 and K7 represent the extremes of commercial compositions for grey irons. Specimen D was in

Figure. 21. Commercial Grey Iron. Specimen 1. x100.

Figure 22. Commercial Grey Iron. Specimen 1. Etched. x400.

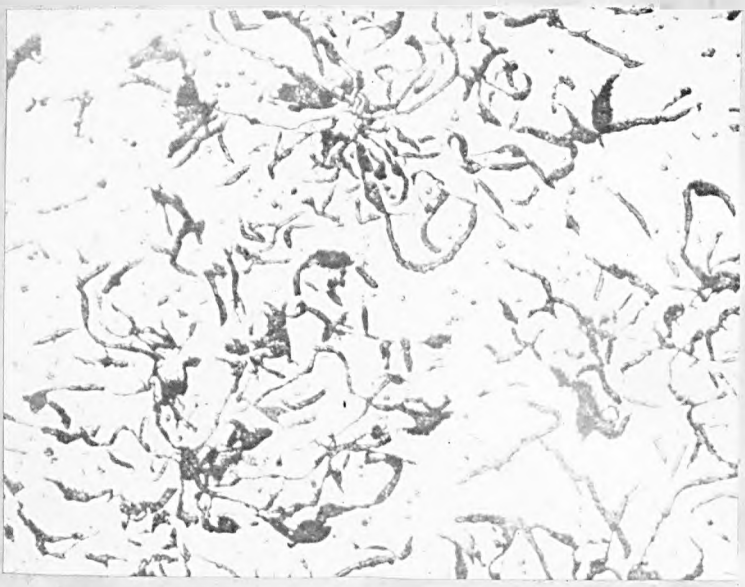

Figure 23. Commercial Grey Iron. Specimen K7. x100.

Figur e 24. Commercial White Iron. Specimen D. Graphite at the centre of the bar. x200.

Figure 25. Commercial White Iron. Specimen D. Carbide near the outside of the bar. x350.

Figure 26, Commercial White Iron. Specimen E. x350.

the form of a 1" diameter chill cast test bar, the centre of which was grey. However, the sample was extracted from the outside of the bar which was white.

The films of extracts from the grey irons all showed strong 0002 Kα and 0002 Kβ graphite lines and the carbide lines were rather faint due to dilution of the specimen with graphite. Efforts were made to separate the carbide from the graphite. As no chemical methods of separation could be devised which would leave the carbide intact, mechanical methods (sieving, blowing with an air stream and froth floatation), were tried but none of these proved successful. Improved results were obtained by using iron radiation instead of cobalt. In some cases a manganese filter was used, but this was omitted when it was found that the only $K\beta$ line which appeared was the graphite line 0002 $K\beta$ and this could not be completely suppressed without unduly reducing the intensity of the $K\alpha$ radiation. Under the best conditions 21 carbide lines were recorded. Examination of the white irons did not prevent any new difficulties.

In all cases the difference between the experiment values of $\sin^2\theta$ and those calculated from the parameters

of cementite disappears as θ approaches 90°. It was not possible to obtain a film which clearly showed the 136 α_1, 251 α_2 and 423.145 overlaps and thus the results cannot be confirmed in the manner employed when examining the films from the high purity specimens.

CONCLUSION AND DISCUSSION

The parameters of the carbide in grey and white irons of normal commercial compositions are the same as those of cementite (Fe_3C).

Most of the commercial irons were examined before the work on the high purity alloys was completed. In view of the fact that the parameters could not be determined with the same high accuracy as that obtained when examining cementite structures, no high angle overlaps being available, it was thought that the results might be attributed to the fact that most of the sulphur and much of the manganese is, in effect, removed by the formation of manganese sulphide (clearly visible in all the microstructures). Thus, the amount of these elements available to enter the carbide is less than that indicated by the chemical composition of the irons and might be insufficient to produce a change in parameters detectable by the methods

employed. However, the work on the high purity alloys has clearly shown that manganese and sulphur, when present in considerable concentrations do not alter the carbide parameters appreciably and thus it is unlikely that this explanation was correct. In fact, the results are completely in accord with the evidence subsequently obtained from the pure alloys.

CARBIDE CONSTITUENTS FOUND IN THE MICROSTRUCTURE OF CERTAIN ABNORMAL IRON-CARBON-SILICON ALLOYS.

I N T R O D U C T I O N

As a result of a detailed microscopic examination of a wide range of iron-carbon-silicon alloys cooled rapidly from the superheated melt, Marles revealed the presence of a constituent intimately associated with the carbide constituent,[11] more resistant to oxidation than the normal carbide, and thus remaining white when the carbide is heat tinted to a dark brown colour. Under the conditions employed by Marles, this new constituent was found, together with the normal carbide, in all alloys containing between 2·5 and 7·0% silicon, and in increasing amounts as the silicon content was raised, and therefore he suggested that it "may be an iron-silico-carbide". During the discussion of Marles' paper[47] we remarked that it was difficult to imagine that the rate of cooling employed in the investigation was sufficient to displace the conditions from equilibrium so far as to cause the formation of one of the complex silico-carbides which are supposed to exist in the equilibrium system with silicon contents

greater than 15%. As an alternative explanation, we suggested that the heat tinting effect may have been produced by segregation of the silicon within a normal carbide phase. This latter view has since been abandoned, more recent work (reported earlier in this thesis) having shown that the normal carbide in white irons is cementite and does not contain any silicon.

Hurst and Riley[12] have reported the presence of a micro-constituent "which has the appearance of cementite" in alloys containing more than 10% silicon. This carbide constituent was found in both sand cast and rapidly cooled alloys. By a metallographic examination of a series of alloys with silicon contents between 10 and 15% and carbon between 1·00 and 0·45%, they, concluded that this phase contained silicon and carbon, but probably with less carbon than "that of normal cementite". If the new constituent described by Marles is a complex silicocarbide it seems to be possible that it may be the same constituent as that described by Hurst and Riley. The work to be described was designed to determine the nature of the two associated "carbide" constituents described by Marles and to discover if

either of these was in fact related to the constituent reported by Hurst and Riley.

ALLOYS CONTAINING 2.5 to 7.0% SILICON

Four of the actual ingots which he used in his earlier investigation were kindly supplied by Mr. Marles. These were treated anodically in a 4% hydrochloric acid electrolyte and the powders irradiated with filtered cobalt radiation in the 19 cm. Debye-Scherrer camera.

All the films were very similar and revealed diffraction patterns with a large number of diffuse lines. The pattern from a sample originally designated by Marles as Melt No.1, Ingot 3, appeared a little clearer than the others. This alloy contained 2·17% carbon and 5·28% silicon and the microstructure of the metal as cast is shown in figure 27. Some improvement in the clarity of the pattern was obtained by sieving this powder to remove the fines and by using a filter between the specimen and the film to reduce the background. Attempts were made to sharpen the lines by annealing. The stability of the two constituents at elevated temperatures had been studied by Marles,

Figure 27. Marles' Iron. Melt No.1. Ingot 3.
As cast. Heat Tinted. x800.

who reported that graphitisation of these alloys proceeds at an appreciable rate at 700°C involving the breakdown of both constituents, the constituent which is resistant to heat-tinting appearing to be the less stable of the two. The powder extracted from alloy Melt No.1.Ingot 3, was annealed for 1 hour at 500°C, in vacuo. The X-ray diffraction pattern now showed quite strong ferrite lines superimposed upon the pattern previously obtained,clearly indicating that decomposition of the alloy had started, but there was no noticeable sharpening of that pattern. As decomposition takes place less readily in the lump than in the powder, it was considered that appreciable stress relief might be effected (before graphitisation set in) if the specimens were annealed before the electrolytic extraction of the powder. The lump specimen was therefore annealed at 600°C for 4 hours. Microscopic examination showed that no graphitisation had taken place, but the diffraction pattern was still not sharpened. A further treatment at 650°C for 2 hours produced some graphitisation, as shown by the microstructure illustrated in figure 28. Most of this graphitisation had started in pearlite areas, which appeared to have grown at the expense

Figure 28. Marles' Iron. Melt No.1. Ingot 3. Annealed . x800.

of both the "carbide" constituents, although a few very small graphite nodules were found remote from the main pearlite areas and associated with the constituent which is responsive to heat tinting. Although the diffraction pattern had been sharpened a little by this treatment it was still more diffuse than the patterns normally obtained from stress free powders under the experimental conditions employed. Most of the clearly distinguishable lines occurred at angles less than 40°, and the highest measurable line was at $64{\cdot}04^{\circ}$. As many of these lines as possible were measured under a travelling vernier microscope. Values of $\sin^2 \theta$ were calculated for 45 lines, but some of the values were somewhat uncertain, especially where groups of broadened lines occurred close together. It was found that 12 lines could be indexed on the basis of the orthorhombic cell of cementite (Fe_3C) and of these lines six of the strongest (121, 210, 022, 103, 113 and 312) were quite clear and well separated from other lines. Details of the results are given in table 6, appendix 3. As no high angle lines of the cementite structure were visible an accurate determination of the unit cell dimensions was not

possible, but the lines obtained were found to give a good fit with the values obtained in the previous work on cementite extracted from high purity iron-carbon-silicon alloys and examined under the same experimental conditions. It is concluded that one of the constituents reported by Marles is normal cementite (Fe_3C) which is in agreement with his conclusion. Further experimental support was obtained by heat tinting the specimen on a mercury bath alongside a high purity iron-carbon-silicon alloy lump specimen of the same size, when it was observed that the cementite in the high purity alloy tinted to the same shade as that constituent in the Marles specimen which had proved sensitive to heat tinting.

When the cementite lines were subtracted an extremely complex pattern remained containing one very strong line at approximately $\theta = 25{\cdot}7^{\circ}$, 5 lines of medium intensity, and a great many weak lines. If all these lines were produced by one constituent, as seems probable from the microscopic evidence, it is clear that the structure must be of low symmetry. Attempts were made to index these lines on the basis of tetragonal and hexagonal unit

cells and of orthorhombic cells of somewhat different dimensions than those of cementite, but they were quite unsuccessful. The pattern was then compared with patterns of the structures of silico-ferrite, the ε and η phase of the iron-silicon system, and the pattern obtained from an iron-carbon-silicon alloy containing a large quantity of the constituent described by Hurst and Riley. The second constituent of the Marles alloy did not appear to bear any resemblence to any of them.

ALLOYS CONTAINING MORE THAN 10% SILICON

An alloy (Specimen A), of composition near to that of the high silicon alloy studied by Hurst and Riley, was prepared by melting high purity iron and silicon, contained in a high purity graphite crucible, in vacuo by means of a high frequency water-cooled coil. After the metal had been molten for about one hour, the input energy to the coil was switched off and the charge cooled fairly rapidly to room temperature, although it is unlikely that the cooling was quite as rapid as that employed by Hurst and Riley. The untreated alloy, which contained 16·5% silicon and 0·52% carbon, gave an X-ray diffraction pattern with strong silico-ferrite

lines, a weak pattern of lines very near to that of the ε phase of the iron-silicon system, and three very weak lines which could be indexed by using the dimensions of the unit cell of the η phase in the iron-silicon system.

As specimen A contained too little of the constituent other than silico-ferrite to produce lines suitable for detailed study another alloy. (Specimen B), containing 24·2% silicon and 0·38% carbon was prepared by melting high purity electrolytic iron powder and silicon (99·92% silicon) in a graphite crucible heated by means of a high frequency unit. The charge was covered with graphite powder and the crucible closed with a graphite lid. The attack on the crucible was severe and as the alloy was molten for 30 minutes it was expected that it would become saturated with carbon. The alloy was cooled slowly by gradually reducing the input to the coil. After sectioning, the specimen was polished with diamond dust and etched in a solution consisting of one part of nitric acid, one part of hydrofluoric acid and 6 parts of water. It was clearly seen that the microstructure (figure 29) contained two constituents which had exactly the same appearance as those obtained by Hurst and Riley in their investigation of

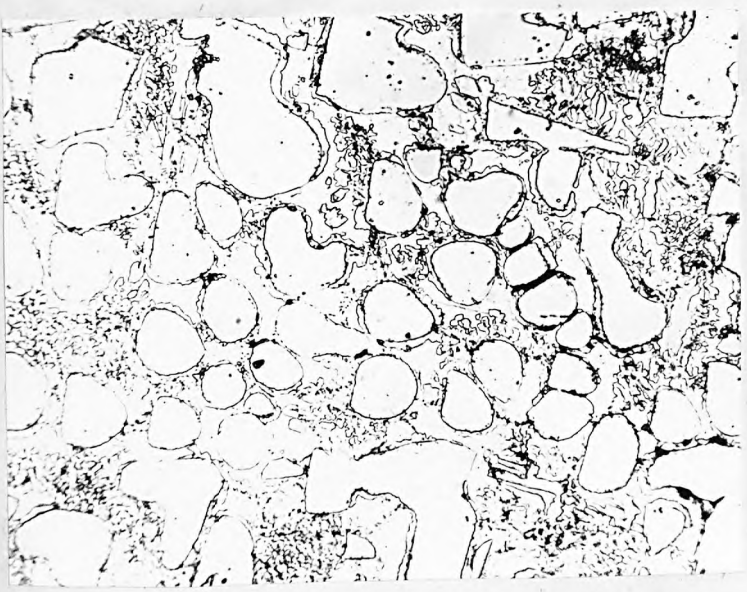

Figure 2 9. High Silicon Fe-C-Si Alloy. Etched in HF/HNO_3 reagent. x300.

the high silicon alloys. The constituent described by them as having "the appearance of cementite" and resistant to etching with sodium picrate was present in large quantities. It was found that this constituent remained unchanged when the specimen was heat-tinted under the same conditions as those employed for the Marles specimen.

A part of the ingot was crushed until it all passed through a 200 mesh sieve and was exposed to filtered cobalt radiation in a 19 cm. camera. The X-ray diffraction pattern obtained was quite clear, although the lines were broadened a little. After annealing the powder for 2 hours at 700°C the lines were sharp and clear and their number, distribution and, as far as could be determined visually, relative intensity, remained unchanged. Details of the reflections observed are given in table 7, appendix 3. All the silico-ferrite lines were clearly visible and calculation by graphical extrapolation method revealed the length of the cube edge of the unit cell to be 2·8183 KX units. If it is assumed that the amount of carbon contained in the silico-ferrite is too small to affect the cell dimensions, then from the data given by Farquhar, Lipson and Weill[54], this

corresponds to a silicon content of 15·1%; which is the composition given by them for the maximum solubility of silicon in the α-phase of the iron-silicon system at temperatures up to 700°C. The alloy was in a condition which probably approximates fairly closely to the equilibrium condition and thus, this observation appears to support the widely held view that the carbon content of high silicon silico-ferrite is very small. As the alloy contains 0·38% carbon, much of this carbon must be contained in the second constituent. This view is in agreement with the results of Hurst and Riley which showed that it contained an appreciable amount of carbon. The remaining strong lines on the diffraction photo-graph were found to correspond to those produced by the ε- phase in the iron-silicon system. The structure of this phase has been fully described by Wever and Möller[55] who showed it to be cubic with four iron and four silicon atoms in the unit cell : It appearing to be a distortion of the Na Cl type of structure. Farquhar, Lipson and Weill found the parameter of the unit cell to be $4{\cdot}4790_5$ KX units in high purity binary alloys. The value of the parameter calculated from the pattern produced by

the Hurst and Riley constituent of the iron-carbon-silicon alloy at present under discussion was found to be 4·4779 KX units, (see table 7, appendix 3). This smaller unit cell size may be due in part to the carbon which has entered the structure, but it is also possible that the silicon content of the constituent is different from that in the binary alloys. All the published equilibrium diagrams show the ε-phase as existing, in the binary system, over a range of silicon content from about 32% to 33·5% silicon.[56] In an earlier determination of the parameter of the unit cell of the ε-phase in iron-silicon alloys Wever and Moller[55] used somewhat impure materials to make up their alloys and obtained a value of 4·467 KX units.

When the silico-ferrite and lines had been indexed all the strong clear lines of the pattern were accounted for, Eight faint low angle lines remained. It was found that these could be indexed on the basis of the η structure of the iron-silicon system, but the lines were all at too low an angle to enable an accurate determination of the parameters of the structure to be made. In the

binary system the η -phase is not a stable phase at room temperature. It is, however, very persistent; very long annealing times being required to cause it to convert to the stable ε-phase. On etching the specimen in the aqueous nitric - hydrofluoric acid reagent it was not possible to distinguish a third microconstituent. The silico-ferrite matrix however has the appearance of a duplex structure (this can also be seen in the photographs produced by Hurst and Riley), and it may be that this is due to the presence of the η -phase. Unfortunately, although the micro-specimen was prepared many times and other etching reagents were tried, it was not possible to discover a technique which clearly showed a third constituent.

CONCLUSIONS.

The conclusions which have been drawn from this work are :-

(1) The constituent, found in rapidly cooled iron-carbon-silicon alloys containing between 2·5 and 7·0% silicon, which is responsive to heat-tinting, is normal cementite (Fe_3C).

(2) The second constituent which is found associated with the cementite in Marles' alloys, and which is

not responsive to heat tinting, has a crystal structure of low symmetry which it has not been possible to determine. However, it has been shown that it is not related to any of the phases found in the iron-silicon or iron-carbon binary systems and, therefore, must be either related to a phase which originates within the ternary system, or be a transition structure induced by the rapid rates of cooling employed. The latter explanation seems the more probable of the two.

(3) The "carbide" constituent described by Hurst and Riley in the high silicon ternary alloys is derived from the ε-phase of the iron-silicon system. The dimensions of the unit cell are, as expected, slightly different from those of the unit cell of the ε-phase, since it contains carbon and possibly has a slightly different silicon content.

(4) The constituent which is resistant to heat-tinting in the alloys investigated by Marles and the constituent reported by Hurst and Riley are not the same.

GENERAL CONCLUSIONS AND DISCUSSION.

The more important conclusions concerning the nature of iron-carbon-silicon alloys, which may be drawn from the present work are:-

1. The carbide phase occurring in high purity alloys has the same structure lattice parameters and composition as cementite (Fe_3C).
2. When manganese is added it mainly enters the austenite or ferrite constituents, although a very small percentage may replace a proportionate amount of iron in the cementite structure.
3. Neither sulphur nor phosphorus enter the cementite.
4. When the alloy is cooled rapidly from the melt the carbide is not plastically deformed but the ferrite is severely strained.
5. The carbide constituent in commercial grey and white irons of normal composition is cementite which does not contain other elements in solution, although it is possible that an insignificant amount of manganese enters the structure.
6. The structure of the constituent associated with

cementite (Marles constituent) in alloys which have been very rapidly cooled from the melt is of low symmetry.

7. The constituent which is designated as "carbide" on microscopic examination of alloys containing more than about 10% silicon is a structure derived from the ε iron-silicon structure by the interstitial substitution of some carbon atoms.

8. The position generally assigned to the peritecto-eutectic point in the metastable iron-carbon-silicon system cannot be correct.

A great many theories have been advanced at different times to account for the relative stability of the carbide and graphite phases under various conditions of temperature and composition. The more important of these have been summarised by Morrough and Williams.[8] Many are highly fanciful and none have found complete experimental support. The problem may be profitably re-examined in the light of the information which has been revealed by the present work. There are two distinct sets of conditions which have to be considered.

1. <u>When the Graphite or Carbide is in Contact with Liquid</u>.

Most of the reliable experimental evidence suggests that when carbon separates under equilibrium conditions it does so in the form of graphite; carbide being formed only as a metastable constituent when the rate of cooling is great and the silicon content low.[79,80.] It is well established that certain addition elements, particularly manganese and chromium, increase the relative stability of the carbide. The relative free energies of the liquid, graphite and carbide phases at a particular temperature will determine which is stable. Attempts to calculate the free-energies of these phases for binary iron-carbon alloys at high temperatures, have not produced consistent results[1,2,3,81,82,83] and, thus, it seems pointless at present to attempt an extension of this work to include the influence of addition elements on the free energy distribution. However, it is now clear that silicon, sulphur and phosphorus exert their influence by altering the relative free-energy of the liquid only. Although manganese may enter the carbide in very small amounts these would be sufficient to produce a large change in the entropy of mixing term and hence in the free-

energy of the carbide. This may be off set to an unpredictable extent by a change in the atomic bonding energy. Most of the manganese enters the liquid and a considerable change in relative free-energy will result. Thus, it is seen that the problem is one of great complexity which is unlikely to be solved from a theoretical point of view until much more experimental data are available and a further advance has been made in our knowledge of the nature of the atomic bonds in this type of crystal.

Other factors influence the solidification to an extent which it is difficult to assess. If it is assumed that the carbide is metastable, then it can only be formed by supercooling the liquid below the solidification temperature of the normal eutectic. Solidification in the stable system will be encouraged by the presence of solid "seed" crystals in the melt. Crystals formed by pro-eutectic solidification will act as "seed" crystals,

but it has also been suggested that other solid particles in the melt may also act in this manner. If this is so, it may be further assumed that certain types of foreign particles nucleate the crystallisation of carbide whilst others nucleate the graphite solidification.

Last month, a paper by Thall and Chalmers[87] appeared in which a new explanation was advanced to explain the undercooling of the aluminium-silicon eutectic when small quantities of sodium are present. It is considered that undercooling of the eutectic liquid is a direct result of a reduction in the solid-liquid interfacial surface tension. They point out that there is a close analogy between the solidification of cast irons and aluminium - silicon alloys and believe "the mechanism of the formation of nodular cast irons to be essentially the same as that described for formation of aluminium silicon alloys". Thus,

if the addition of certain elements can cause a change in the habit of the graphite crystals by altering the interfacial surface tension resulting in an alteration in the degree of undercooling of the eutectic liquid, it is clear that this must also be an important factor when considering the relative stability of graphite and carbide.

2. When Graphite or Carbide is in Contact with Austenite.

When a white iron is annealed to produce malleable iron, it contains at the annealing temperature carbide in contact with austenite at the start of the operation and graphite in contact with austenite at the end. It is often assumed that the graphite is produced by direct decomposition of the carbide and that the influence of silicon, manganese and sulphur may be explained in terms of their effect upon the stability of this constituent. In the case of silicon and manganese, it is generally supposed that this influence is exerted by these elements entering the carbide structure. Further, a number of investigators report that the composition

of the carbide varies over a wide range of carbon content, either during the annealing treatment or when this treatment is performed at different temperatures[84,85,86]. These theories are elaborated to the greatest degree by Schwartz, Van Horn and Junge[84] in a paper in which, having described attempts to measure the carbon content of the carbide phase under different conditions by means of planimeter measurements of the carbide areas on microsections and by the crude X-ray methods already described, they summarise the changes which occur on annealing a white iron in the following terms:

"1. Alpha iron has changed to gamma iron.

2. Some carbon or cementite has gone into solution in gamma iron to form a solid solution. ----

3. Some cementite has been decomposed into carbon and gamma iron and the carbon atoms have displaced iron atoms, iron atoms, resulting from both reactions becoming the solvent for forming more solid solution, still further reducing the amount of cementite. Possibly there is a limiting carbon concentration in cementite, which may or may not be reached before all the carbon finally crystallizes out

as graphite. The compound Fe_2C often referred to may represent merely the resulting maximum solubility corresponding to the substitution of one carbon atom for one iron atom in every unit cell.

4. With increasing temperature (and time?) carbon atoms leave the cementite cell to crystallize out in the free state. This depletion may go even to the point of removing some of the atoms originally required in the Fe_3C arrangement before the structure changes to gamma iron throughout".

The present work has shown that any such theory is untenable. Although it is possible that the small amount of manganese which enters the carbide may stablise this structure, it is clear that the main influence of silicon, manganese, ~~sulphur~~ and phosphorus is exerted by virtue of the fact that these elements enter the austenite. Microscopic examination shows that the graphite forms within the austenite whilst there is no evidence to suggest that cementite precipitates graphite directly. As graphitisation proceeds the cementite dissolves in the austenite, thus replenishing the carbon content.

It has been established by Norbury and others that austenite in contact with cementite is supersaturated

with carbon in respect to the equilibrium concentration in austenite in contact with graphite. Thus, at a temperature at which diffusion can take place at an appreciable rate, graphite nuclei will form and grow within the austenite. For the reaction to start however graphite nuclei must form; the reaction potential is supplied by the difference in the free-energies of austenite in contact with graphite and that of the original austenite. This difference will be influenced to a pronounced extent by the nature and quantity of other elements dissolved in the austenite. Binary iron-carbon alloys containing carbon in the form of cementite do not graphitise easily. It is reasonable to asume that elements (X) which restrict the austenite range in the ternary iron-carbon-X systems increase the free-energy of the austenite to a pronounced extent and thus provide a greater reaction potential and facilitate graphitisation, whilst those elements which enlarge this range will have the reverse effect. This would explain the action of manganese, silicon and phosphorus. The latter has only a small graphitising action due to its

restricted solubility in austenite.

Sulphur acts in a more complex manner. The solubility of this element in gamma iron is less than ·025% and this figure is further reduced by the presence of carbon and silicon. Williams [88] has recently shown that very small percentages of sulphur have a graphitising effect when present in iron-carbon alloys. However, larger quantities have the reverse effect and in pure iron-carbon-silicon alloys even small quantities of sulphur act as a carbide stabiliser. The insoluble sulphur appears in these alloys as iron sulphide (Fe S) and the carbide stabilising effect is associated with the presence of this compound. In cast irons of commercial compositions the influence of the sulphur dissolved in the austenite appears to be insignificant: the important factor being the nature of the compound formed by the insoluble sulphur. This reacts with the manganese present.

$$Fe\,S + Mn \rightleftharpoons M_nS + Fe$$

The extent to which the reaction approaches completion depends upon the percentage of

manganese available. Morrough[89] showed that when iron sulphide predominates in the structure it acts as a carbide stabiliser and the graphite which ultimately forms on annealing is of the flake aggregate variety, whilst manganese sulphide acts as a graphitising agent and promotes the formation of the nodular form of graphite. At present no explanation can be advanced to account for these phenomena.

Marle's discovery of a new constituent associated with the cementite in certain white irons leads to interesting speculation as to the possibility of the existence of a transition structure in the cementite decomposition process and the possible connection between such a intermediate structure and the graphitisation of a solid phase at temperatures just below the melting point, which is thought to produce the distinctive type D graphite, when irons of a suitable composition are cooled from the liquid. However, at present there are insufficient data to permit any deductions to be drawn. Further work is in hand which is designed to provide this necessary information.

APPENDIX 1.

THE BRADLEY 19 cm. POWDER CAMERA.

The cameras used in the investigation were of the standard pattern produced by Unicam Instrument Co. Ltd. with 4·0mm. x 1·0 mm. collimating slits. The constructional details of this type of camera are shown in the figure 30.

A BACK REFLECTION CAMERA FOR USE WITH METALLOGRAPHIC SPECIMENS

Although the camera was designed and constructed for the specific purpose described in the thesis, it is capable of much wider application. With the increasing application of Debye-Scherrer methods to problems in the field of classical metallography, the need arises for an experimental method which will enable results of high accuracy to be obtained directly from a micro-specimen, thus eliminating the uncertainty which sometimes exists when X-ray results obtained from powdered specimens are correlated with microstructures. Methods have been devised for the microexamination of these powder specimens, but the technique is difficult and tedious, and the results obtained are sometimes difficult to interpret. It is obviously more satisfactory

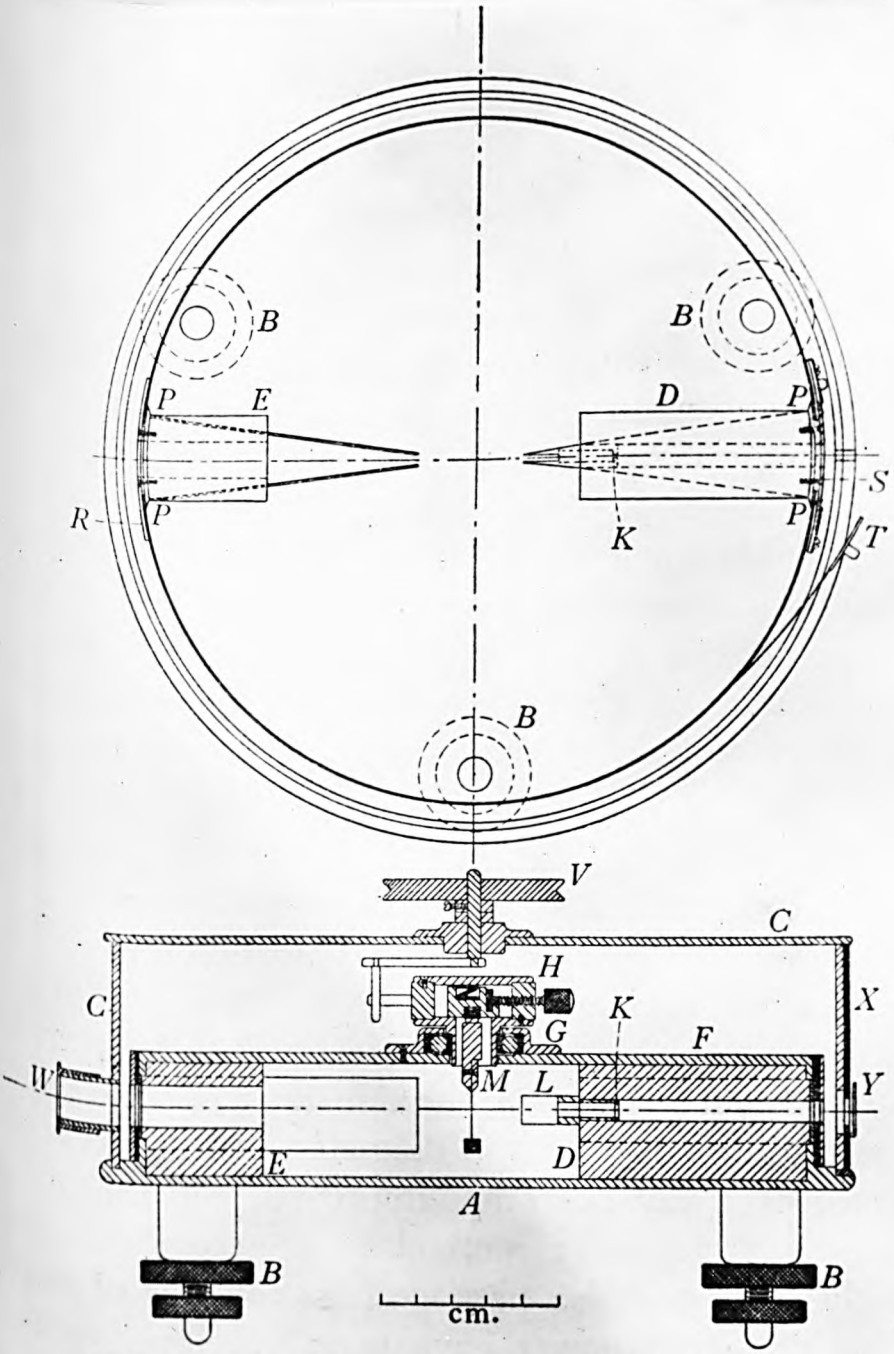

FIG. 38.—Plan and vertical section of 19-cm. camera.
(A. J. BRADLEY, *Journal of Scientific Instruments*, 18, 1941.)

Figure 30.

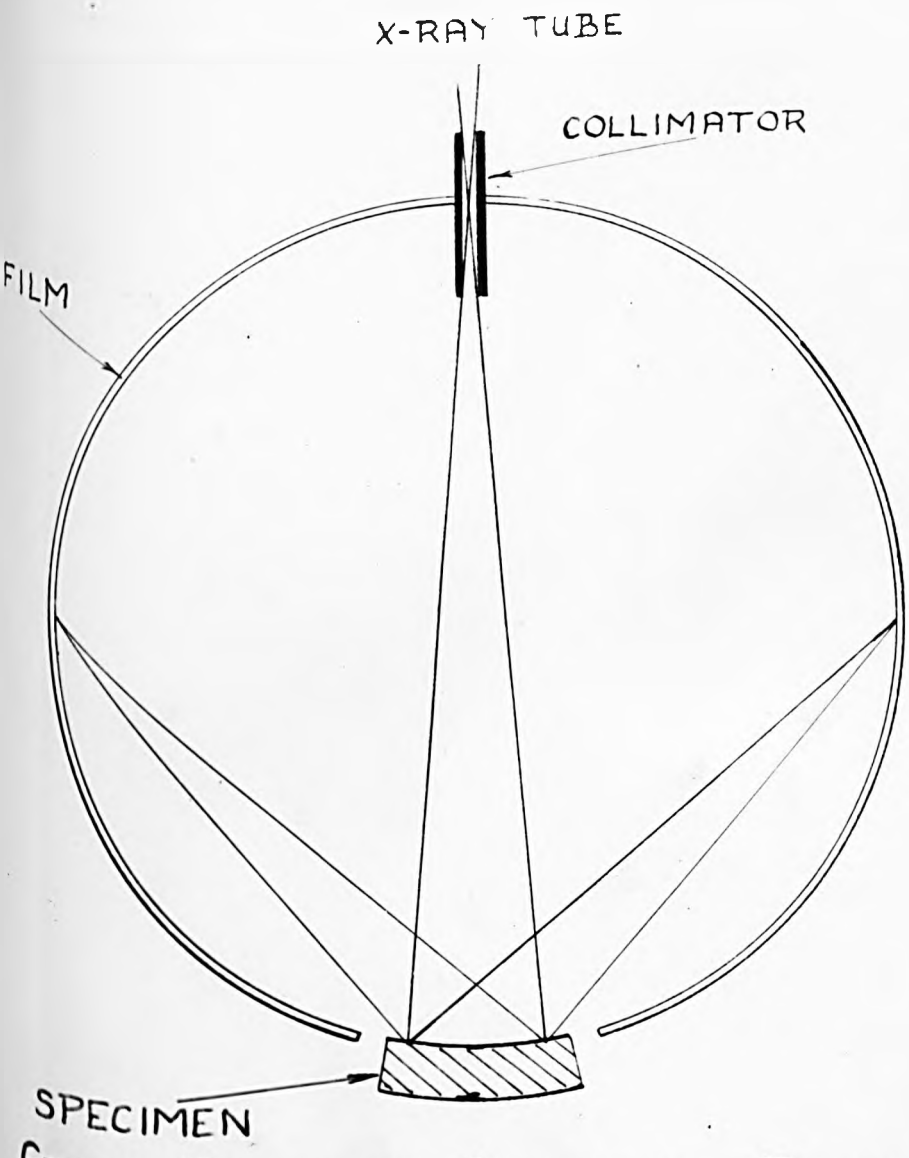

GENERAL PRINCIPLE OF SYMMETRICAL FOCUSING

to use a normal micro-specimen for X-ray examination. To obtain a Debye-Scherrer pattern from such a specimen requires a back reflection technique. The usual flat plate arrangement is open to two major objections: only a very small section of the pattern is recorded and hence it is not possible to identify the structures present without reference to some other source of information, and secondly, it is not usually possible to achieve the high degree of accuracy of lattice parameter measurements which can be obtained by the powder methods, there being insufficient lines to allow the use of extrapolation methods for the elimination of systematic error. A wider range of Bragg angle θ can be recorded with symmetrical focusing back reflection cameras [14,57,58]. and Jette and Foote [61] have demonstrated that cameras built on this principle are capable of producing results of the same accuracy as the best powder methods. Figure 31 shows the general experimental arrangement and demonstrates the focusing principle. In all the cameras which have been described a widely divergent beam has been used necessitating the use of a specimen with the exposed surface curved to the contour of the film circle. Generally a specimen in the form of a powder

adhering to the surface of a suitably formed templet has been used (eg. Owen et. al.[60,61]). Gaylor and Preston[58] have used a poly-crystalline solid sheet formed to the required profile but with such an arrangement, only linear motion parallel to the major axis of the film cylinder, or tangentially in a plane normal to that axis, is possible. In neither case can the motion be produced with the necessary accuracy by a simple mechanical mechanism. Thus, it is usual to use a stationary specimen and to arrange for a large number of the power particles to be exposed in order that continuous lines may be produced. When stationary polycrystalline specimens are used the lines are spotty and of poor definition (see photograph reproduced by Gaylor and Preston[58]).

The camera, about to be described, has provision for rotating the specimen and thus gives continuous lines. The microspecimen is etched, to remove the strained surface layer produced by the polishing operations, before it is loaded into the camera. The flat surface does not, of course, fit the profile of the film cylinder but, provided the irradiated breadth of the specimen is small compared with the distance from the focal point of the beam to the specimen, no

appreciable broadening of the line will result from this cause. As will be shown later, the flat surface results in a small error in the measurement of the angle θ ,but this can be allowed for. With the large specimen - focus distance (4") employed in the present camera, it was found in practice that quite large beam divergence could be allowed without increasing the breadth of the lines beyond that normally encountered in powder cameras of the Bradley type. This allowed considerable reductions in the exposure time, Sharper lines may be obtained by using smaller collimators and less divergent beams but with a correspondingly longer exposure. Thus, the choice of collimator, and hence exposure, is determined by the accuracy that is required.

CONSTRUCTIONAL DETAILS

Working drawings of the camera are shown in figure 33 and 34. The specimen is held in position with a suitable spring with the surface automatically located so that it lies normal to that diameter of the film cylinder which passes through the collimator and tangentially to the imaginary horizontal circle containing the film. A small electric motor rotates the specimen at a speed of 1 revolution per minute.

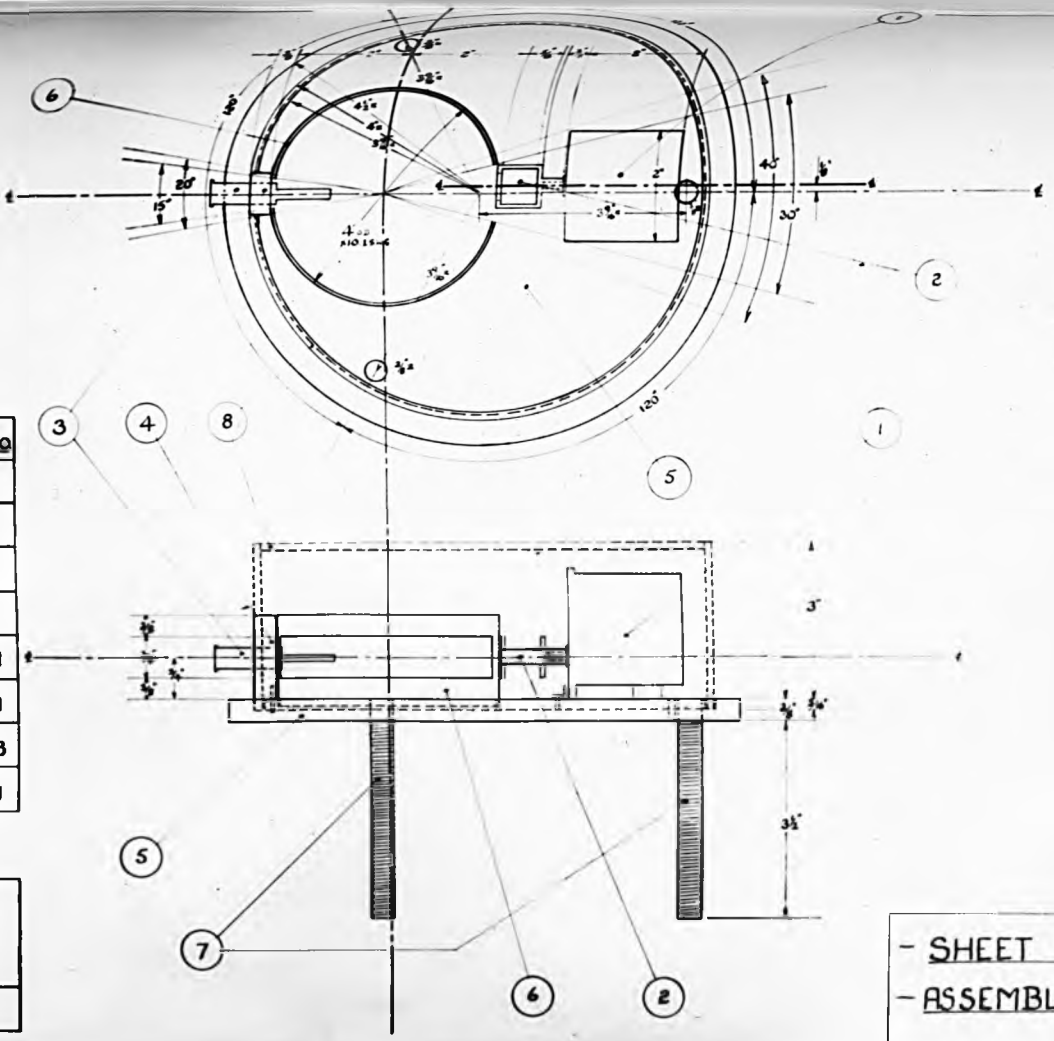

ITEM	DESCRIPTION	MATL.	No
1	ELECTRIC MOTOR		1
2	SPECIMEN HOLDER	BRASS	1
3	COLLIMATOR	BRASS	1
4	COLLIMATOR HOLDER	BRASS	1
5	BASE PLATE	BRASS	1
6	FILM HOLDER	BRASS	1
7	SCREWED RODS 3/8" UNIT.	STEEL	3
8	COVER	STEEL	1

- X-RAY BACK REFLECTION FOCUSING CAMERA -

DEPARTMENT OF METALLURGY
UNIVERSITY OF LIVERPOOL

- SHEET 1 -
- ASSEMBLY -

Figure 33.

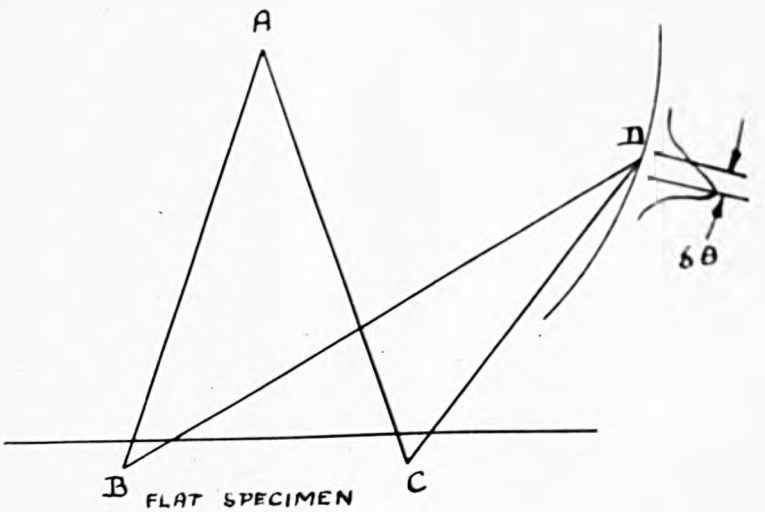

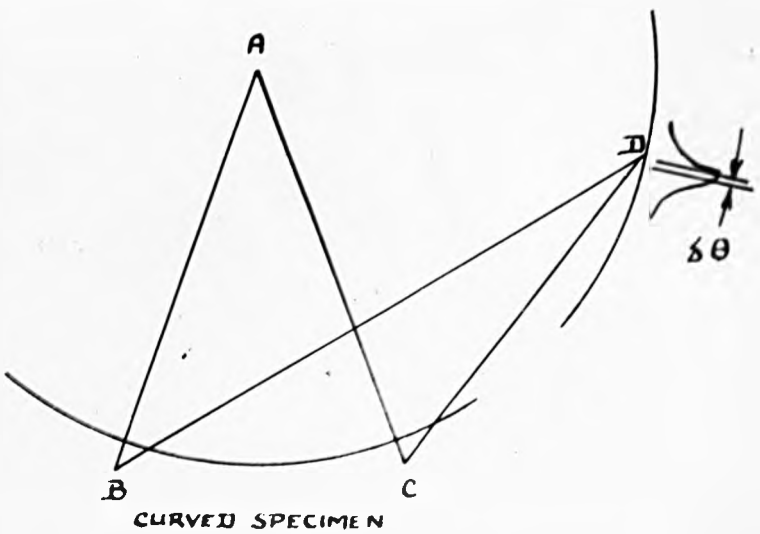

DIAGRAMMATICAL REPRESENTATION OF ABSORPTION ERROR DUE TO FLAT SURFACE

Figure 32.

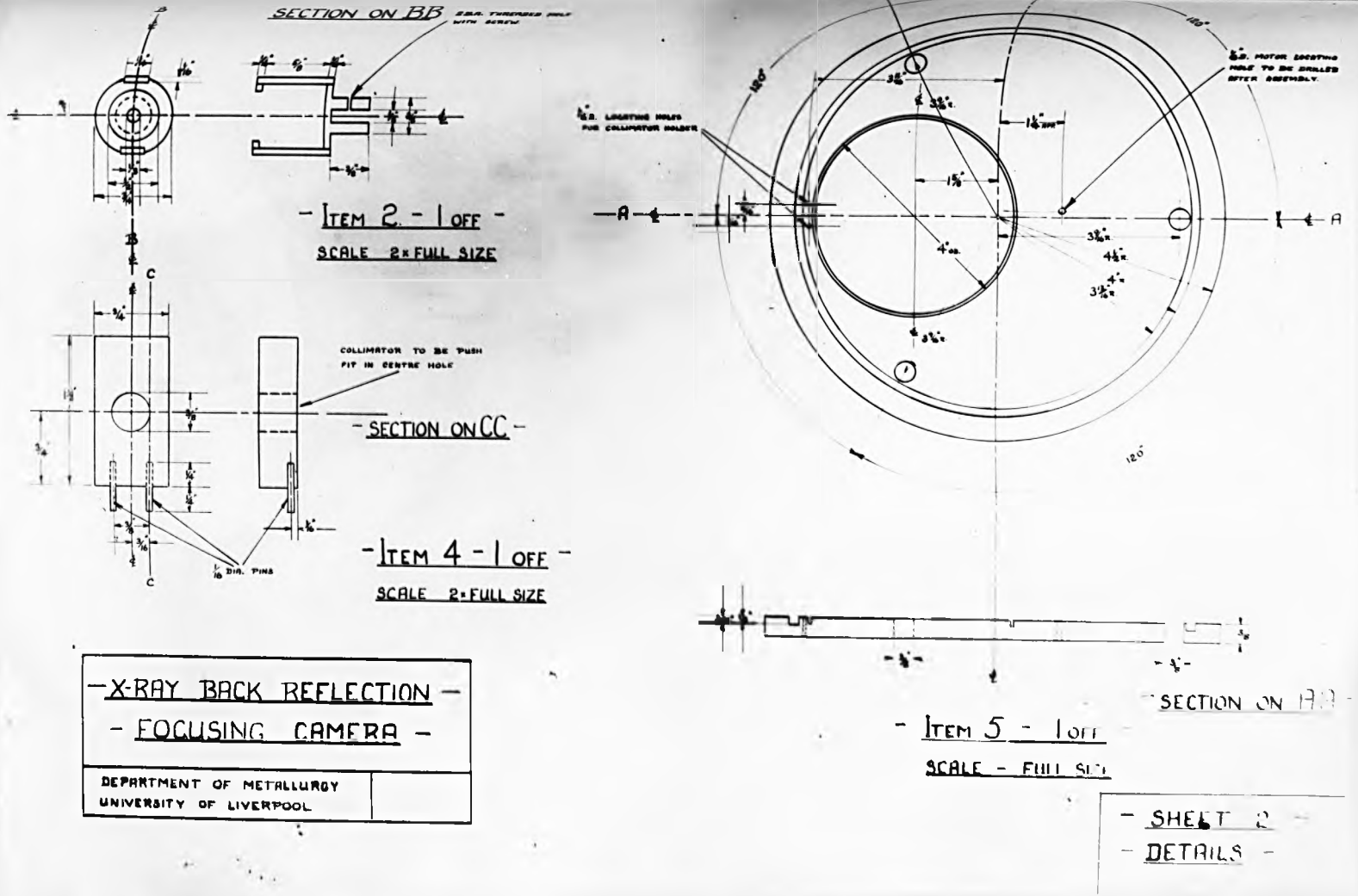
SECTION ON BB
- ITEM 2. - 1 OFF -
SCALE 2× FULL SIZE
COLLIMATOR TO BE PUSH FIT IN CENTRE HOLE
- SECTION ON CC -
- ITEM 4 - 1 OFF -
SCALE 2× FULL SIZE
- ITEM 5 - 1 OFF
SCALE - FULL SIZE
- X-RAY BACK REFLECTION -
- FOCUSING CAMERA -
DEPARTMENT OF METALLURGY
UNIVERSITY OF LIVERPOOL
- SHEET 2 -
- DETAILS -

Figure 34.

The axis of rotation is parallel to, but displaced $\frac{1}{8}$" from, the diameter through the collimator, so that when the specimen is rotated the surface is scanned by the X-ray beam. The drawings (figures 33 and 34) show the collimator locating block held in position by two plugs. This arrangement had to be modified later as it proved very difficult to drill the holes for the plugs in exactly the correct positions. One plug was removed and a small arm carrying a screw was fixed to the opposite side of the block, so that it could be swivelled on the plug until correctly aligned and then clamped to the base plate by means of this screw. When setting up the collimator the specimen was replaced by a fluorescent screen with a line $\frac{1}{8}$" off-centre scribed on it. A number of different slit sizes were tried out and ultimately it was decided that the best combination for most purposes was the one shown in figure 35. The position of the focal point within the collimator tube was calculated and the collimator position adjusted so that this point lay on the film circle; small final adjustments had to be made by trial and error.

The film holder is in two halves, as in the Bradley 19 cm. powder camera; the film being held in position

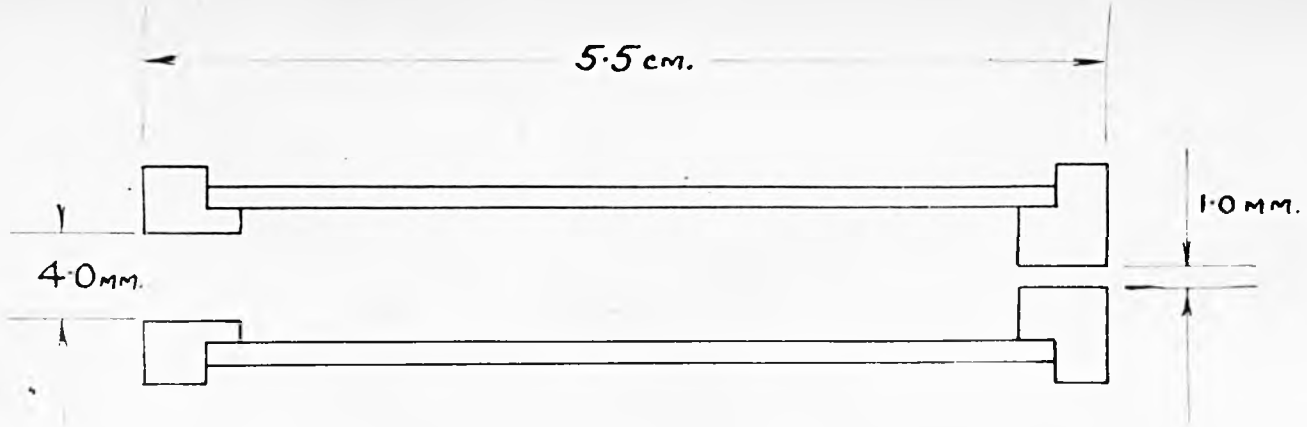

DIMENSIONS OF COLLIMATOR

Figure 35.

by elastic bands. The knife edges are positioned so that a range of Bragg angle from 55° to 82° can be recorded. Some films that have been obtained with this camera are shown in figure 36.

METHOD OF CALCULATION.

The Bragg angle θ is obtained in the following manner:

Referring to figure 37, let

D - Diameter of film circle. Measured with micrometer.

S_{HA} - Arc distance between high angle knife edges. Calculated from micrometer measurements of linear distance.

S_{LA} - Arc distance between low angle knife edges. Calculated from micrometer measurement of linear distance.

S_1 and S_2 - Distances from line to high angle knife edge shadow on the film. Measured on travelling microscope.

ST1 and ST2 - Total distances between knife edge shadows measured on the film.

1. Ferrite - Annealed Pure Iron.
2. Ferrite - Fe-C-Si Alloy, Specimen P.
3. Pure Silicon.

Figure 36.

HIGH ANGLE KNIFE EDGES

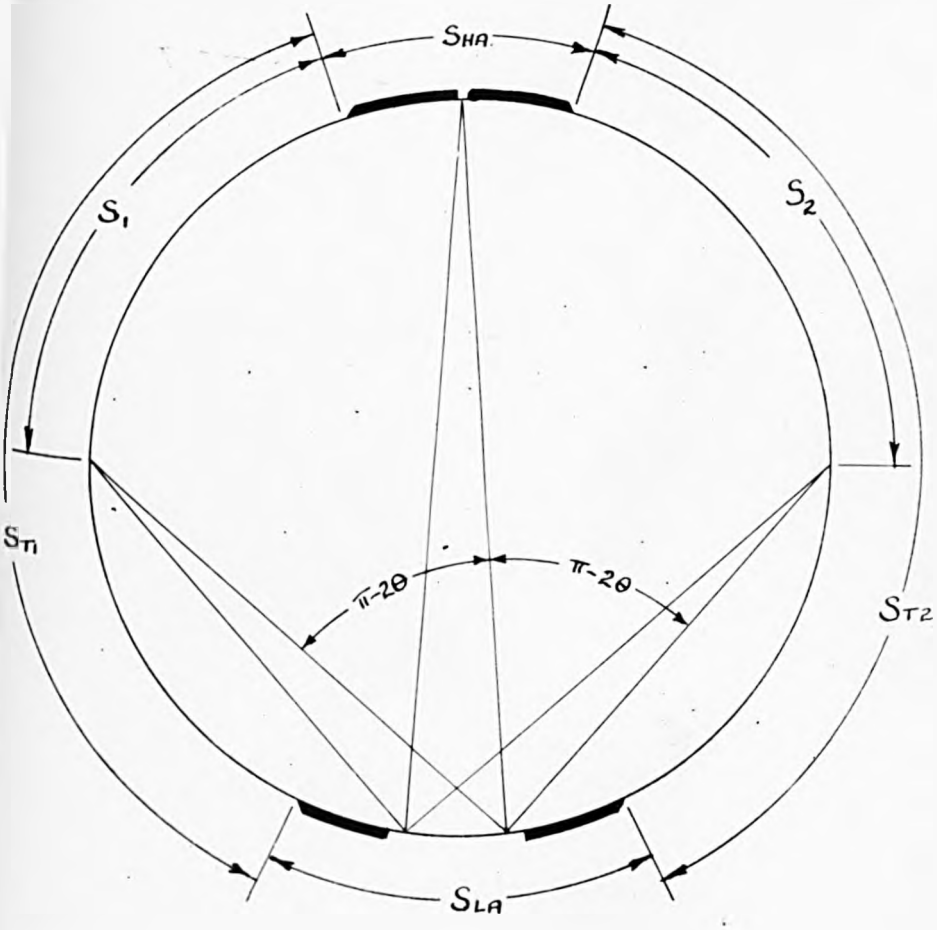

MEASUREMENTS FOR CALCULATION OF θ

Figure 37.

A correction for film shrinkage may be made separately on each film by simple proportion, thus

$$\frac{S1}{ST1} = \frac{Sc1}{\pi D - (SHA + SLA)}$$ where Sc1 - corrected value of S1.

$$Sc1 = \frac{S_1 [\pi D - (SHA + SLA)]}{ST1} \quad \text{- - - - - - - - - - - - - - - (1)}$$

similarly

$$Sc2 = \frac{S2 [\pi D - (SHA + SLA)]}{ST2} \quad \text{- - - - - - - - - - - - - - - (2)}$$

where Sc2 = Corrected value of S2

$[\pi D - (SHA \quad SLA)]$ is a constant of the camera.

In practice it was found that this error was so small, since the camera design permits short films to be used, that it can usually be neglected.

The total arc distance between the lines = Sc1 + Sc2 + SHA

Let this expression = S

The angle subtended at the centre of the camera by the arc S = $4(\pi - 2\theta)$.

Thus

$$\frac{S}{\pi D} = \frac{4(\pi - 2\theta)}{2\pi}$$

hence

$$\theta = \frac{\pi}{2} - \frac{S}{4B} \quad \text{- - - - - - - - - - - - - - - (3}$$

As $\mathcal{D}$ is a constant which can be determined with great accuracy, appreciable error in θ can only be produced by an error in the measurement of S.

Combing equation (3) with the Bragg equation

$$d = \frac{\lambda}{2} \cdot \operatorname{Sec} \frac{S}{4\mathcal{D}}$$

and since $d = a\, f(h.k.l)$ where a = length of cube edge of unit cell of a cubic structure h.k.l. = Miller indices.

$$\frac{\delta d}{d} = \frac{\delta a}{a} = \tan \frac{S}{4\mathcal{D}} \cdot \delta\left(\frac{S}{4\mathcal{D}}\right)$$

If $\frac{S}{4\mathcal{D}}$ is small, as it is at high angles of reflection,

$$\frac{\Delta a}{a} = \left(\frac{S}{4\mathcal{D}}\right)^2 \cdot \frac{\Delta S}{S} \qquad \text{- - - - - - - - - - - (4)}$$

i.e. the percentage error in a is obtained by multiplying the percentage error in S by the square of a small number less than unity and will thus be very small and will decrease rapidly as S becomes smaller, i.e. as θ approaches 90^0.

Further, by considering the individual sources of error in S, and hence in θ, it will now be shown that these rapidly approach zero as θ approaches 90^0.

The error in S arises due to the following causes:

1. The geometrical error, due to misalignment of the beam relative to the specimen and film and variation of the specimen film distance during rotation of the specimen. (For detailed analysis of these errors in flat plate back reflection cameras see Lu and Chang [63]). As the camera was accurately constructed, it is considered that these errors are negligably small when it is properly set up.

2. Absorption error. As shown in figure 32, the difference between the distances travelled within the specimen by beams ABD and ACD is very small when the specimen surface is curved to the profile of the film circle, but is much larger when, as in the present case, a flat specimen is used. Hence, the maximum of the intensity curve will not occur at the geometrical centre of the line, and thus there will be a tendency to measure a value of S which is greater than the true value. It is clear from the diagram that this total path difference becomes smaller as θ increases and disappears when $\theta = 90^{\circ}$.

3. Error due to double coating on the film. As the films generally used have a coating on each

side, there is some displacement of the images when the reflected beam strikes the film at an oblique angle. This effect is only noticeable when θ is less than 60°.

Bradley and Jay[36], and Taylor and Sinclair[39] have shown that the extent of the shift of the lines due to absorption by a cylindrical powder specimen may be deduced from first principles when the volume and shape of the specimen is known. Such analysis is not possible in this case as the depth of penetration of the beam cannot be estimated with certainty. It was thus necessary to find a relationship between θ and the error in parameter measurement by empirical methods. Films were taken of specimens of tin, lead, silicon, and iron and in each case the parameters were plotted against θ. All the curves were of the general form shown in figure 38. At angles greater than 76° the curves became almost horizontal. It is clear from these curves that results of the same order of accuracy as those obtained by the Bradley method can be achieved simply by plotting the parameter values against θ and extrapolating to $\theta=90^{\circ}$. It is, of course, necessary to have at least two lines in the

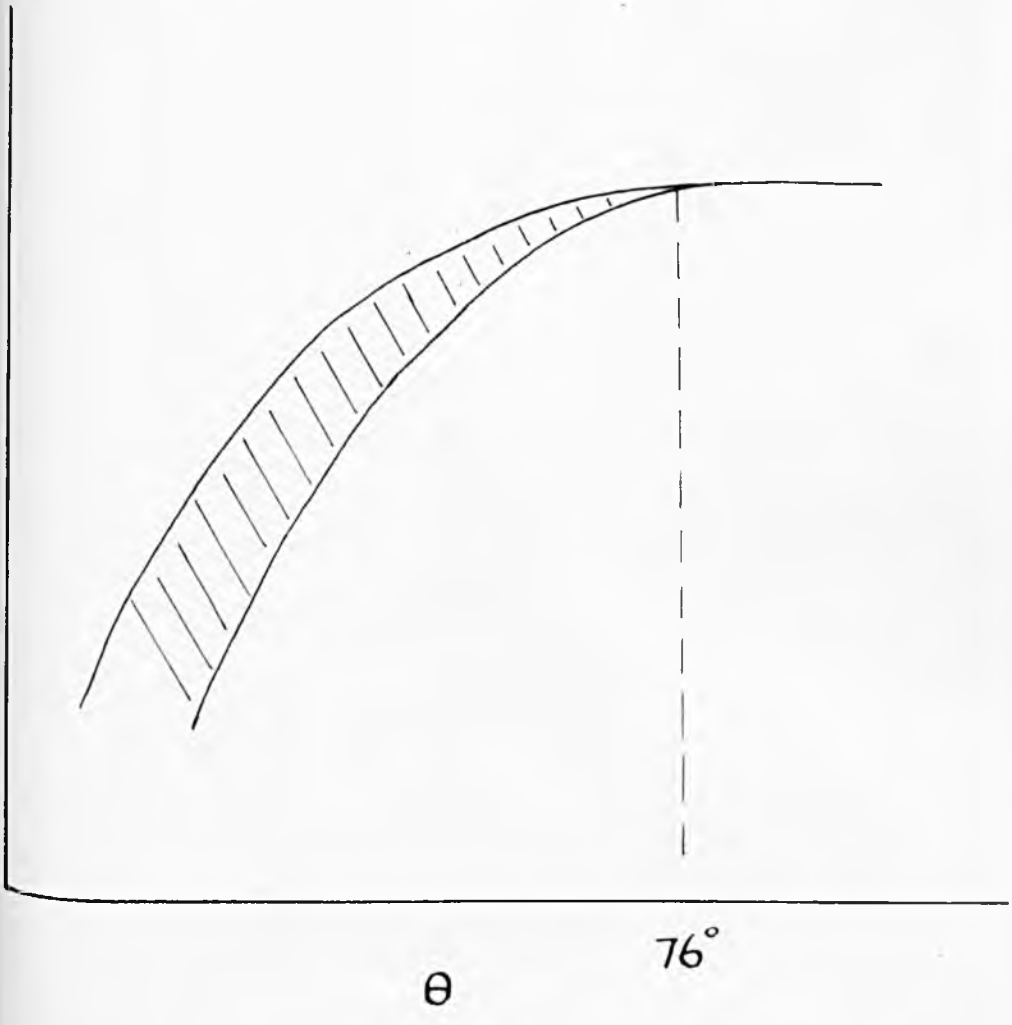

General Form of a/θ Rot.

Figure 38.

range $\theta = 76^0$ to $\theta = 82^0$, but this restriction seldom presents any difficulty as it can be overcome by the choice of a radiation of suitable wavelength. In fact, the parameters given by lines in this range are estimated to be correct to within $\pm$ 0·00005 Å, which is of the same order of accuracy as that achieved by the best Bradley methods and therefore further correction is unnecessary. The results obtained from experiments on a Hilger iron sample are given below to illustrate this point.

A. Cylindrical annealed powdered specimen in 19 cm Unicam Bradley Camera. Parameter plotted against $\cos^2\theta$ and extrapolated to $\theta = 90^0$. Average of three films :-

$$a = 2{\cdot}8610_2$$

B. Flat annealed lump specimen in back reflection focusing camera:

$S^\dagger$	θ	$\sin^2\theta$	Index	$\frac{\sqrt{N}.\lambda.}{2.}$	a.
6·11	81·41	·9777	310 $_2$	2·82896	2·86100
6·66	80·64	·9735	310	2·82279	2·86094
19·56	62·37^0	·7850	220 $_2$	2·53030	2·85607
19·81	62·16	·7819	220	2·52478	2·85509
26·839					

$\dagger$ S was corrected for film shrinkage

$$a = 2{\cdot}8610_0$$

CONCLUSION

An X-ray diffraction camera has been developed which can be used to obtain parameter measurements directly from the surfact of a normal microspecimen. The accuracy achieved is comparable with that obtained by using a 19 cm. Bradley camera and a powdered specimen. A sufficient angular range of the pattern is recorded to enable most structures to be identified without resort to subsidiary methods of examination.

A P P E N D I X 2.

TABLE 1.

Values of $\sin^2\theta$ for Cementite (Fe_3C) Structure.

Calculated from the parameters a - 4·5155 Å

b - 5·0773 Å

c - 6·7265 Å

Only the lines considered by Lipson[16] (L), Petch[22] (P) and Hume-Rothery and others[17] (HR) are listed.

Index	$\sin^2\theta$	(Cobalt K mean)
020	·12376	(L)
112)	·14059)	(L)
021)	·14138)	
200	·15664	(L)
120	·16290	(L)
121	·18055	(L)
210	·18758	(L)
022	·19425	(L)
103	·19775	(L)
211	·20521	(L)
113	·22869	(L)
122	·23341	(L)
212	·25807	(L)
004)	·28193)	(L)
023)	·28235)	
130	·31763	(L)

Index	$\sin^2\theta$	(Cobalt K mean).
140	·53421	(P)
313	·54198	(P)
025	·56429	(P)
233	·59370	(P)
125	·60345	(P)
	$\sin^2\theta$	
235 K α_1	·87427	(HR)
235 K α_2	·87807	(HR)
152 K α_1	·88179	(HR)
152 K α_2	·88562	(HR)
107 K α_1	·90119	(HR)
430 K α_1	·90363	(HR)
334 K α_1)	·91143)	(HR)
423 K α_2)	·91145)	
251 K α_1	·94710	(HR)
251 K α_2)	·95122)	(HR)
136 K α_1)	·95130)	
136 K α_2	·95543	(HR)
145 K α_1)	·97322)	(HR)
153 K α_2)	·97397)	
432 K α_1)	·97400)	
145 K α_2)	·97743)	(HR)
432 K α_2)	·97823)	

TABLE 2.

ALL POSSIBLE REFLECTIONS FOR IRON PHOSPHIDE (Fe_3P) STRUCTURE

Structure - tetragonal, Space Group S_4^2.

Calculated from parameters given by Taylor[78].

Values of $\sin^2\theta$ for Cobalt K α mean :-

h,k	l				
	0	1	2	3	4
0,0	-	-	·1612	-	·6448
0,1	-	·0500	-	·3724	-
1,1	·0194	-	·1806	-	·6642
2,0	·0388	-	·2000	-	·6836
2,1	-	·0888	-	·4112	-
2,2	·0776	-	·2388	-	·7224
3,0	-	·1276	-	·4500	-
3,1	·0970	-	·2582	-	·7418
3,2	-	·1664	-	·4888	-
4,0	·1552	-	·3164	-	·8000
4,1	-	·2052	-	·5276	-
3,3	·1746	-	·3358	-	·8194
4,2	·1940	-	·3552	-	·8388
4,3; 5,0	-	·2828	-	·6052	-
5,1	·2522	-	·4134	-	·8970
5,2	-	·3216	-	·6440	-
4,4	·3104	-	·4716	-	·9552
5,3	·3298	-	·4910	-	·9746
6,0	·3492	-	·5104	-	·9940
6,1	-	·3992	-	·7216	
6,2	·3880	-	·5492	-	

h,k	l				
	0	1	2	3	4
5,4	-	·4380	-	·7604	
6,3	-	·4768	-	·7992	
7,0	-	·5156	-	·8380	
8,5;7,1	·4850	-	·6462	-	
6,4	·5022	-	·6634	-	
7,2	-	·5521	-	·8745	
7,3	·5601	-	·7213	-	
6,5	-	·6294	-	·9518	
8,0	·6180	-	·7792	-	
8,1;7,4	-	·6680	-	·9904	
8,2	·6557	-	·8179		
6,6	·6953	-	·8565		
8,3	-	·7453	-		
7,5	·7145	-	·8758		
8,4	·7726	-	·9338		
9,0	-	·8225	-		
9,1	·7919	-	·9531		
9,2;7,6	-	·8611	-		
8,5	-	·8998	-		
9,3	·8691	-			
9,4	-	·9770			
7,7	·9464	-			
10,0: 8,6	·9657				
10,1	-				

APPENDIX 3.

TABLE 1.

RESULTS from IRON-CARBON ALLOY SPECIMEN 1. FILM 353

S	θ	$\sin^2\theta$	Index	$\Delta \sin^2\theta \times 10^{-4}$
14·67	22·122	1417	021·112	+ 3
15·50	23·374	1573	200	+ 7
15·83	23·872	1637	120	+ 8
16·72	25·214	1814	121	+ 9
17·05	25·711	1882	210	+ 7
17·41	26·254	1956	022	+ 13
17·54	26·450	1984	103	+ 6
17·90	26·993	2060	211	+ 8
18·98	28·622	2294	113	+ 8
19·21	28·969	2345	122	+ 10
20·29	30·597	2591	212	+ 10
21·33	32·166	2835	004·023	+ 11
21·98	33·146	2990	221	+ 10
22·81	34·397	3192	130	+ 16
23·52	35·468	3367	131	+ 14
24·15	36·418	3524	114	+ 4
26·13	39·404	4029	311	+ 19
28·14	42·435	4554	312	+ 16
29·13	43·928	4813	105	+ 17
31·20	47·040	5356	140	+ 14
31·50	47·502	5436	313	+ 16
31·88	48·075	5537	141	+ 19

TABLE 1 (Continued)

S	θ	$\sin^2\theta$	Index	$\Delta \sin^2\theta \times 10^{-4}$
32·37	48·814	5663	025	+ 20
33·50	50·518	5957	233	+ 20
33·86	51·061	6050	125	+ 15
34·91	52·644	6318	330	+ 9
35·94	54·196	6578	410	+ 3
36·30	54·740	6668	314	+ 15
38·58	58·179	7220	225	+ 11
40·18	60·591	7588	324,135, 026	± 0
40·63	61·270	7689	421	+ 9
45·99	69·353	8757	235 α_1	+ 14
46·25	69·745	8802	235 α_2	+ 21
46·44	70·029	8833	152 α_1	+ 15
46·63	70·315	8865	152 α_2	+ 9
47·59	71·766	9021	107 α_1	+ 9
48·23	72·728	9119	334 α_1, 423 α_2	+ 5
50·92	76·784	9477	251 α_1	+ 6
51·28	77·330	9519	251 α_2 136 α_1	+ 6
51·64	77·873	9559	136 α_2	+ 5
53·54	80·736	9741	145 α_1, 153 α_1, 432 α_1	+ 2
54·03	81·474	9780	145 α_2 432 α_2	+ 2
56·582				

TABLE 1 (Continued)

RESULTS FROM IRON-CARBON-SILICON ALLOY - SPECIMEN 2 FILM 383

S	θ	$\sin^2\theta$	Index	$\Delta \sin^2\theta \times 10^{-4}$
14·66	22·083	1413	021, 112	0
15·50	23·348	1571	200	+ 5
15.82	23·830	1632	120	+ 3
16·72	25·186	1812	121	+ 6
17·05	25·683	1878	210	+ 2
17·57	26·466	1987	103	+ 9
17·89	26·948	2054	211	+ 2
19·02	28·650	2298	113	+11
19·21	28.936	2342	122	+ 8
20·28	30·548	2584	212	+ 3
21·34	32·145	2832	004, 023	+ 8
21·99	33·124	2985	221	+ 4
22·78	34·314	3178	130	+ 2
23·53	35·444	3363	131	+ 10
24·16	36·393	3519	114	-1
26·10	39·315	4015	311	+ 5
26·28	39·586	4061	024	+ 4
28·13	42·373	4542	312	+ 3
31·20	46·997	5349	140	+ 7
31·50	47·449	5427	313	+ 7
32·37	48·760	5654	025	+ 11
33·46	50·401	5937	233	0
33·85	50·989	6038	125	+ 3

TABLE 1 (Continued)

S	θ	$\sin^2 \theta$	Index	$\Delta \sin^2\theta \times 10^{-4}$
34·90	52·571	6306	330	-3
35·05	52·797	6345	304	+ 1
35·82	53·956	6538	043	+ 1
35·94	54·137	6569	410	+ 6
36·29	54·664	6654	314	+ 1
36·68	55·252	6751	411	0
38·59	58·129	7213	225	+ 4
41·64	62·723	7899	324,135, 026	+ 11
46·01	69·306	8752	235 α_1	+ 9
46·22	69·622	8787	235 α_2	+ 6
46·44	69·954	8825	152 α_1	+ 7
47·63	71·746	9020	107 α_1	+ 8
50·98	76·794	9478	251 α_1	+ 7
51·32	77·306	9518	251 α_2 136 α_1	+ 5
51·67	77·833	9555	136 α_2	+ 1
53·60	80·740	9740	145 α_1 153 α_2 432 α_1	+ 3
54·09	81·478	9781	145 α_2 432 α_2	0
56·670				

TABLE 1 (Continued)

RESULTS FOR IRON-CARBON-SILICON ALLOY, SPECIMEN 3. FILM 379.

S	θ	$\sin^2\theta$	Index	$\Delta\sin^2\theta \times 10^{-4}$
14·64	22·048	1409	112·021	0
15·46	23·283	1562	200	-4
15·80	23·795	1628	120	-1
17·04	25·663	1876	210	0
17·39	26·190	1948	022	+ 5
17·56	26·446	1984	103	+ 6
17·89	26·943	2051	211	-1
18·98	28·584	2288	113	+ 1
19·20	28·916	2339	122	+ 5
20·28	30·542	2582	212	+ 1
21·33	32·124	2827	004·023	+ 3
22·03	33·178	2995	221	+ 15
22·78	34·307	3178	130	+ 2
23·51	35·407	3358	131	+ 5
24·17	36·401	3521	114	+ 1
28·15	42·395	4547	312	+ 8
31·21	47·003	5349	140	+ 7
31·51	47·455	5429	313	+ 9
31·93	48·088	5538	141	+ 20
32·37	48·750	5653	025	+ 10
33·48	50·422	5940	233	+ 3

TABLE 1 (Continued)

S	θ	$\sin^2\theta$	Index	$\Delta \sin^2\theta \times 10^{-4}$
33·89	51·039	6047	125	+ 12
34·93	52·606	6313	330	+ 4
36·03	54·263	6588	410	+ 13
36·33	54·715	6664	314	+ 11
80·93	76·702	9471	$251\alpha_1$	0
81·33	77·306	9518	$251\alpha_2$ $136\alpha_1$	+ 5
81·69	77·848	9557	$136\alpha_2$	+ 3
86·681				

TABLE 2.

RESULTS FOR IRON-CARBON-SILICON-MANGANESE ALLOY A.

SPECIMEN M1. FILM 421

S	θ	$\sin^2\theta$	Index	$\Delta \sin^2\theta \times 10^{-4}$
32·42	48·802	5661	025	+ 18
33·61	50·593	5969	233	+ 32
33·93	51·074	6052	125	+ 17
36·06	54·280	6592	410	+ 17
43·34	65·239	8246	315 α_1	+ 20
51·38	77·341	9520	136 α_1, 251 α_2	+ 07
51·74	77·884	9559	136 α_2	+ 05
86·682				

SPECIMEN M2. FILM 423.

S	θ	$\sin^2\theta$	Index	$\Delta \sin^2\theta \times 10^{-4}$
32·51	48·949	5688	025	+ 45
33·67	50·696	5988	233	+ 51
33·98	51·163	6067	125	+ 32
36·13	54·400	6611	410	+ 36
43·34	65·256	8249	315 α_1	+ 23
51·46	77·482	9530	136 α_1, 251 α_2	+ 17
86·668				

TABLE 2 (Continued)

SPECIMEN M3. FILM 429

S	θ	$\sin^2\theta$	Index	$\Delta \sin^2\theta \times 10^{-4}$
32·50	48·908	5681	025	+ 38
33·58	50·534	5959	233	+ 22
33·92	51·046	6049	125	+ 14
36·08	54·296	6595	410	+ 20
43·32	65·192	8240	315 α_1	+ 14
51·54	77·562	9536	136 α_1, 251 α_2	+ 23
51·87	78·059	9572	136 α_2	+ 18
56·725				

TABLE 3.

RESULTS FOR IRON-CARBON-SILICON ALLOY CONTAINING SULPHUR

SPECIMEN S1. FILM 425

S	θ	$\sin^2\theta$	Index	$\Delta \sin^2\theta \times 10^{-4}$
32·39	48·755	5654	025	+ 11
33·52	50·456	5947	233	+ 10
33·88	50·999	6040	125	+ 5
34·84	52·443	6284	215	+ 3
35·03	52·729	6333	304·323	+ 10
36·04	54·248	6586	410	+ 11
43·26	65·117	8230	315 α_1	+ 4
51·33	77·264	9514	136 α_1, 251 α_2	+ 1
51·72	77·851	9557	136 α_2	+ 3

θ_k 56·712

TABLE 4.

REFLECTIONS FROM EXTRACT OF IRON-CARBON-SILICON ALLOY CONTAINING PHOSPHORUS

SPECIMEN P1. FILM 424.

S	θ	$\sin^2\theta$	Index	
11·53	17·363	0890	$21\bar{3}1$	Iron Phosphide Structure
13·93	20·978	1282	$30\bar{3}1$	"
15·99	24·080	1654	$32\bar{5}1$	"
16·37	24·652	1740	$33\bar{6}0$	"

TABLE 4. (Continued)

S	θ	$\sin^2\theta$	Index	
16·71	25·164	1808	$11\bar{2}2$	Iron Phosphide Structure
17·35	26·128	1939	$42\bar{6}0$	"
17·89	26·941	2053	$41\bar{5}1$	"
19·45	29·290	2393	$22\bar{4}2$	"
20·00	30·119	2516	$51\bar{6}0$	"
20·30	30·570	2586	$31\bar{4}2$	"
21·33	32·121	2827	$43\bar{7}1$ $50\bar{5}1$	"
26·03	39·199	3995	$61\bar{7}1$	"
28·98	43·642	4763	$63\bar{9}1$	"
29·52	44·455	4906	$53\bar{8}2$	"
30·97	46·639	5286	$41\bar{5}3$	"
31·94	48·099	5540	$72\bar{9}1$	"
33·93	51·096	6057	$43\bar{7}3$, $50\bar{5}3$	"
34·91	52·572	6306	$65\ \bar{1}1\ 1$	"
35·49	53·445	6453	$64\bar{10}2$, $55\bar{10}2$, $71\bar{8}2$	"
36·26	54·605	6646	$11\bar{2}4$	"
39·70	59·785	7468	$83\bar{1}1\ 1$	"
42·96	64·695	8174	$82\bar{1}0\ 2$	"
43·97	66·216	8375	$70\bar{7}3$	"
45·22	68·098	8609	$92\bar{1}1\ 1$, $76\bar{1}3\ 1$	"
45·93	69·167	8735	$72\bar{9}3$	"
47·47	71·486	8992	$85\ \bar{1}3\ 1$	"
51·32	77·284	9515	$65\ \bar{1}1\ 3$	"
53·86	81·109	9762	$94\ \bar{1}3\ 1$	"
55·86	84·121	9894	$81\bar{9}3$, $74\ \bar{1}1\bar{3}$	"

S_k 56·658

TABLE 5.

RESULTS FROM IRON-CARBON-SILICON ALLOY CONTAINING PHOSPHORUS

SPECIMEN P2. FILM 182.

S	θ	$\sin^2\theta$	Index	$\Delta\sin^2\theta \times 10^{-4}$
32·38	43·717	5647	025	+4
33·53	50·446	5946	233	+ 9
33·90	51·004	6040	125	+ 3
34·87	52·462	6287	215	+ 6
36·05	54·237	6585	410	+ 10
43·28	65·115	8230	315 α_1	+ 4
51·37	77·286	9516	136 α_1 251 α_2	+ 3
51·73	77·828	9555	136 α_2	+ 1

TABLE 6.

RESULTS FROM MARLE'S IRON. MELT No.1 INGOT 3.

FILM 187.

S	θ	$\sin^2\theta$	Index	
13·68	20·612	·1239		
14·60	21·998	1403	112. 021	Cementite
15·26	22·993	1526		
15·69	23·640	1608		
15·97	24·062	1662		
16·71	25·177	1810	121	Cementite
17·06	25·705	1882	210	"
17·37	26·172	1945	022	"
17·55	26·443	1983	103	"
18·98	28·598	2291	113	"
19·28	29·050	2358		
19·63	29·577	2437		
19·87	29·939	2491		
20·39	30·722	2610		
20·96	31·581	2743		
21·22	31·973	2803		
21·69	32·681	2916		
21·92	33·027	2971	221	Cementite
22·30	33·600	3062		
22·56	33·992	3125		
24·04	36·222	2491		

TABLE 6 (Continued)

S	θ	$\sin^2 \theta$	Index	
24·75	37·291	3670		
26·79	40·365	4196		
27·85	41·962	4472		
28·10	42·339	4536	312	Cementite
28·84	43·454	4730		
29·07	43·800	4791		
29·81	44·915	4986		
31·08	46·829	5319		
31·39	47·296	5401		
31·80	47·914	5507		
32·06	48·305	5577		
32·34	48·727	5649	025	Cementite
32·64	49·179	5727		
32·96	49·661	5810		
33·14	49·933	5856		
33·49	50·460	5947	233	Cementite
36·57	55·100	6726		
39·21	59·078	7360		
39·36	59·304	7393		
39·98	60·239	7536		
40·44	60·932	7640		
40·62	61·203	7679		
42·50	64·036	8034		

56·655

TABLE 7

RESULTS FOR HIGH SILICON IRON-CARBON-SILICON ALLOY

SPECIMEN B. FILM 410.

θ	$\sin^2\theta$	Index	θ	$\sin^2\theta$	Index
15·649	0727	110 η	41·525	4396	311 ε
16·568	0813	110 ε	46·071	5187	320 ε
18·044	0959	200 η	48·337	5582	321 K α_1 ε
18·631	1020	111 η	48·480	5606	321 K α_2 ε
20·394	1214	111 ε	51·019	6043	211 K α_1 α-Fe
20·981	1282	201 η	51·169	6069	211 K α_2 α-Fe
22·427	1456	002 η	52·945	6369	400 ε
23·662	1611	200 ε	55·367	6771	410,322 ε
24·054	1661	110K β α-Fe	57·804	7160	411,330 ε
24·325	1697	102 η	60·377	7557	331 K α_1 ε
26·743	2025	110 α-Fe	60·588	7588	331 K α_2 ε
27·473	2128	300 η	63·732	8041	220 K α_1 α-Fe
27·714	2162	112 η	63·973	8074	220 K α_2 α-Fe
29·400	2410	211 ε	66·049	8353	421 K α_1 ε
35·621	3392	200 K β α-Fe	66·320	8387	421 K α_2 ε
36·856	3598	300,221 ε	69·254	8745	332 K α_1 ε
39·470	4041	200 α-Fe	69·585	8784	332 K α_2 ε

θ	Index	N	$\sqrt{N}\lambda/2.$	cosec θ	a
60·377	331 Kα_1	19	3·89095	1·150355	4·47597
60·588	331 Kα_2	19	3·89945	1·147960	4·47639
66·049	421 Kα_1	21	4·09061	1·094220	4·47603
66·320	421 Kα_2	21	4·09955	1·091938	4·47645
69·254	332 Kα_1	22	4·18688	1·069336	4·47718
69·585	332 Kα_2	22	4·19602	1·067018	4·47722

Extrapolation against $\sin^2\theta$ gives parameter of $\mathcal{E}$- structure as

$$a = 4{\cdot}4779_5$$

A P P E N D I X 4.

COMPOSITIONS OF MATERIALS USED FOR PREPARING THE ALLOYS

1. HILGER IRON, J.M.845

Nickel	0·0076 %
Copper	0·0002%
Manganese	Trace
Silicon	Faint trace
Aluminum	Faint trace

No other elements were detected by spectrographic analysis.

2. ELECTROLYTIC IRON SHEET

Principal impurities:

Phosphorus	0·015 %
Copper	0·01 %

3. SILICON - St.Lawrence Metals and Alloys Ltd.

Silicon	99·80 per cent
Iron	0·006 " "
Aluminium	0·022 " "
Manganese	Nil
Copper	Nil
Calcium	0·006 " "
Titanium plus Zirconium	0·003 " "
Phosphorus	0·005 " "
Cobalt	Nil
Nickel	Nil
Carbon	0·01 " "

4. CARBON

Total ash content 0·07%

E-ray analysis showed the major constituents of the ash to be Ca O and $CaSO_4$

REFERENCES

1. E. Jänecke: Zeitschrift für Metallkunde, 1940,vol.32, p.142.

2. E.Jänecke: Zeitschrift für Metallkunde, 1941, vol.33, p.186.

3. Yap, Chu-Phay and Liu: Transactions of the Faraday Society, 1932, vol.28, p.788.

4. K.Honda, K.Iwase and K.Sano: Science Report Tohoku Imperial University, 1936, vol.25, p.202.

5. H.Morrough: Journal of Iron and Steel Institute, 1941, vol. 143, p.195.

6. J.T.Eash: Transactions of American Foundrymen's Association, 1941, vol.49, p.887.

7. American Society for Testing Materials: "Tentative Recommended Practice for Evaluating the Microstructure of Graphite in Grey Iron". Designation: A 247 - 41 - T.

8. H. Morrough and W.J.Williams: Journal of the Iron and Steel Institute, 1947, vol.155, p.321.

9. H.Morrough and W.J.Williams: Journal of Iron and Steel Institute, 1948, vol. 158, p.306.

10. H.A.Schwartz, K.R.Van Horn and C.H.Junge: Transactions of American Society for Steel Treating; 1933, vol.21, p.463.

11. D.Marles: Journal of the Iron and Steel Institute, 1948, vol. 158, p.433.

12. J.E.Hurst and R.V.Riley: Journal of Iron and Steel Institute, 1944, vol.149, p.213.

13. A.Westgren: Journal of Iron and Steel Institute,1921, vol.103, p.303.

14. A. Westgren and G.Phragnèn: Journal of Iron and Steel Institute, 1922, vol.105, p.241.

15. B.Hendricks: Zeitschrift für Kristallographie, 1930, vol. 74, p.534.

16. H.Lipson and N.J.Petch: Journal of Iron and Steel Institute, 1940, vol.142, p.95.

17. W.Hume-Rothery, G.V. Raynor and A.T.Little: Journal of Iron and Steel Institute, 1942, vol.145, p.143.

18. J.E.Hurst and R.V.Riley: Journal of Iron and Steel Institute, 1944, No.I p.221.

19. W.Wrazej: Journal of Iron and Steel Institute, 1944, No I. p.227.

20. J.E. Hurst and R.V.Riley: Journal of Iron and Steel Institute, 1945, No.I p.105.

21. A. Westgren, H. Phragmèn and Negresco: Journal of Iron and Steel Institute, 1928, vol.117, p.383.

22. N.T.Petch: Journal of Iron and Steel Institute, 1944, vol.144, p.143.

23. Seventh Report on the Heterogeneity of Steel Ingots, Iron and Steel Institute, 1937, Special Report No.16.

24. Colbeck, S.W. Craven and W.Murray : Journal of Iron and Steel Institute, 1941, vol.143, p.332.

25. E.W.Colbeck and S.W.Craven: Journal of Iron and Steel Institute, 1943, vol.148, p.243.

26. T.E.Rooney: Seventh Report on the Heterogeneity of Steel Ingots, Iron and Steel Institute 1937 Special Report No.16, p.113.

27. T.E. Rooney: Eighth Report on the Heterogeneity of Steel Ingots, Iron and Steel Institute 1939, Special Report No.25, p.142.

28. T.E. Rooney: Journal of Iron and Steel Institute,1941, vol. 143, p.344.

29. T.E.Rooney: Journal of Iron and Steel Institute, 1943 vol.148, p.248.

30. E.Taylor-Austin: Eighth Report on the Heterogeneity of Steel Ingots, Iron and Steel Institute 1939, Special Report No.25, p.121.

31. E. Taylor - Austin: Journal of Iron and Steel Institute, 1941, vol. 143, p.358.

32. J.G.Pearce: Journal of Iron and Steel Institute, 1941, vol. 143, p.366.

33. W.Westwood: Journal of Iron and Steel Institute, 1943, vol. 148, p.278.

34. D.J.Blickwede and Morris Cohen: Journal of Metals, 1949, vol.1 No.9, p.578.

35. A.J.Bradley, H.Lipson and N.J.Petch: Journal of Scientific Instruments, 1941, vol.18,p.216.

36. A.J.Bradley and A.H.Jay: Proceedings of the Physical Society, 1932, vol. 144, p.563.

37. H.Lipson and A.J.C.Wilson: Journal of Scientific Instruments, 1941, vol.18. p.216.

38. T.B.Nelson and D.P.Riley: Proceedings of the Physical Society, 1945, vol.57, p.160.

39. A.Taylor and H.Sinclair: Proceedings of the Physical Society, 1945, Vol.57, p.126.

40. K.Honda and T.Murakami: Journal of Iron and Steel Institute, 1923, vol.107. p.545.

41. D.Hanson: Journal of Iron and Steel Institute,1927, vol.116, p.129.

42. H.Sawamura: Memoirs of the College of Engineering, Kyoto Imperial University, 1926,vol.4, No.4.

43. E. Scheil: Stahl u. Eisen. 1930, vol.50, p.1725.

44. E. Scheil: Stahl u. Eisen, 1932, vol.52, p.129.

45. A. Kříž and F.Pobořil: Journal of Iron and Steel Institute, 1932, vol. 126, p.323.

46. A. Kříz and F.Pobořil: Journal of Iron and Steel Institute, 1930, vol.122, p.191.

47. W.Shepherd Owen: Journal of Iron and Steel Institute, 1948, vol. 160, p.21.

48. W.Shepherd Owen and B.G.Street, submitted to Iron and Steel Institute. April 1950 Not yet published.

49. T.Satô: Technical Reports of Tohoku Imperial University, 1930, vol.9. p.515.

50. W.Gontermann: Journal of Iron and Steel Institute 1911. vol. 83, p.421.

51. K. Honda and T. Murakami: Science Reports of Tohoku Imperial University, 1924, vol.12, p.257.

52. H. Hanemann and H.Jass: "Anniversary Volume Dedicated to K. Honda", Tohoku Imperial University, 1936, p.793.

53. H. Hanemann and H.Jass: Giesserie, 1938, vol.25 p.293.

54. M.C.M. Farquhar, H.Lipson and A.R.Weill: Journal of Iron and Steel Institute, 1945, vol.152, p.457.

55. F.Wever and H. Moller: Zeitschrift für Kristallographie 1930, vol.75, p.362.

56. "Metals Handbook": American Society for Metals, Cleveland, 1939, p.396.

57. E. A. Owen and E.L.Yates: Philosophical Magazine, 1934. vol. 17, p.113.

58. M. Gayler and G.D.Preston: Journal of Institute of Metals, 1929, vol. 41. p.191.

59. E.A.Owen and J.Iball: Philosophical Magazine, 1932, vol.13 p.1020.

60. E.A.Owen, Pickup and Roberts: Zeitschrift fur Kristallographie, 1935, vol.91. p.70.

61. E.R.Jette and F.Foote: Journal of Chemical Physics, 1935, vol.3, p.605.

63. S.S.Lu and Chang: Proceedings of Physical Society, 1941.

64. Arnold and Reed: Journal of Iron and Steel Institute, 1910, vol. 38, p.169.

65. B.Jacobson and A.Westgren: Zeitschrift für Physikalische Chemie, 1933, vol.20, p.361.

66. H.J.Goldschmidt: Journal of Iron and Steel Institute, vol. 160, p.345.

67. M.Gensamer: Transactions of American Society for Steel Treating, 1933, vol.21, p.1028.

68. E.C.Bain, E.S. Davenport and W.S.N.Waring: Transactions of American Institute of Mining and Metallurgical Engineers, Iron and Steel Division, vol. 100, p.228.

69. R.Vogel and W.Doring: Archiv fur das Eisenhuttenwesen 1932, vol.6, p.35.

70. F.M.Walters and C.Wells: Transactions of the American Society for Steel Treating, 1933, vol.21, p.830; Transactions of the American Society for Metals, 1935, vol.23, p.751.

71. M.Gaylor: Journal of Iron and Steel Institute, 1933, vol. 128, p.293; N.P.L. Collected Researches, 1935.

72. F.M.Walters: Transactions American Society for Steel Treating, 1932, vol.19, p.577.

73. H.Hanemann and A.Schildkotter: Archiv fur das Eisenhuttenwesen, 1929, vol.3. p.427.

74. R.Vogel and G.Ritzau: Archiv fur das Eisenhüttenwesen, 1931, vol. 4. p.549.

75. T. Satô: Technical Reports of Tohoku Imperial University, 1932, vol. 10, p.453.

76. R.Vogel: Archiv fur das Eisenhuttenwesen, 1929, vol.3, p.369.

77. M.Künkele: Mitteilungen aus dem Kaiser-Wilhelm Institut fur Eisenforschung zu Dusseldorf, 1930, vol.12. p.23.

78. A.Taylor, "X-ray Metallography", London, 1945, p.371.

79. C.Wells: Transactions of the American Society for Metals, 1936, vol. 26. p.289.

80. H.A. Schwartz: Transactions of American Society for Metals, 1935, vol.23, p.126.

81. K.K.Kelley: "Thermodynamic Properties of Metal Carbides and Nitrides", U.S.Bureau of Mines Bulletin, 1938, No.407.

82. W.A. Roth: Z. angew. Chem., 1929, vol.42, p.981.

83. H.Naeser: Mitteilungen aus dem Kaiser - Wilhelm Institut fur Eisenforschung zu Dusseldorf 1934, vol.16. p.1.

84. H.A.Schwartz, K.R.Van Horn and C.H.Junge: Transactions of American Society for Steel Treating, 1933, vol.21, p.463.

85. H.A.Schwartz, H.H.Johnson and C.H.Junge: Transactions of American Society for Steel Treating, 1930, vol.17, p.383.

86. A.A.Bates and D.E.Lawson: Transactions of American Society for Steel Treating, 1930, vol.18 p.659.

87. B.M.Thall and B.Chalmers: Journal of Institute of Metals, 1950, vol.77, p.79.

88. W.H.Williams: Journal of Iron and Steel Institute, 1950, vol.164, p.407.

89. H.Morrough: Journal of Iron and Steel Institute, 1946, vol. 154. p.399.